COMPONENT PART NOTICE

THIS PAPER IS A COMPONENT PART OF THE FOLLOWING COMPILATION REPORT:

TITLE: _Microwave Antennas for Avionics. Lecture Series of the_ ~~Panel~~ _Avionics Panel and the Consultant and Exchange Programme Held in Rome, Italy on 7-8 May 1987; Guenzburg, Germany on 11-12 May 1987 and Ankara, Turkey on 14-15 May 1987._

TO ORDER THE COMPLETE COMPILATION REPORT, USE ___AD-A185152__.

THE COMPONENT PART IS PROVIDED HERE TO ALLOW USERS ACCESS TO INDIVIDUALLY
AUTHORED SECTIONS OF PROCEEDING, ANNALS, SYMPOSIA, ETC. HOWEVER, THE COMPONENT
SHOULD BE CONSIDERED WITHIN THE CONTEXT OF THE OVERALL COMPILATION REPORT AND
NOT AS A STAND-ALONE TECHNICAL REPORT.

THE FOLLOWING COMPONENT PART NUMBERS COMPRISE THE COMPILATION REPORT:

AD#: _P005 663_   AD#: _P005 670_

AD#: _____   AD#: _____

AD#: _____   AD#: _____

Accession For	
NTIS GRA&I	☒
DTIC TAB	☐
Unannounced	☐
Justification	
By_____	
Distribution/	
Availability Codes	
Dist	Avail and/or Special
A-1	

DTIC
SELECTED
OCT 2 8 1987
E

DTIC FORM 463
MAR 85

OPI: DTIC-TID

DISCLAIMER NOTICE
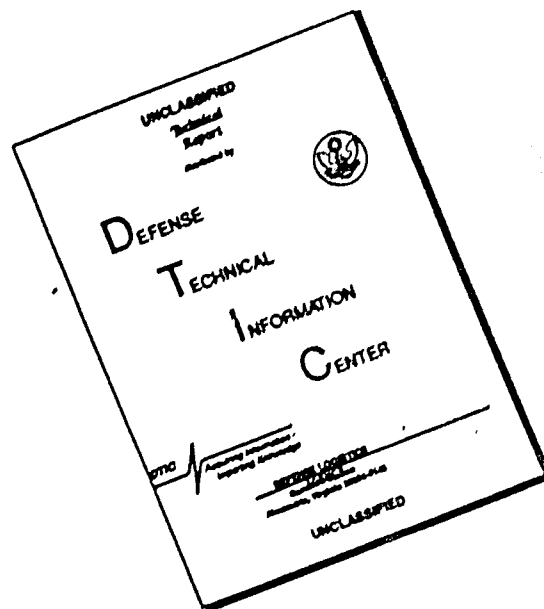
THIS DOCUMENT IS BEST QUALITY AVAILABLE. THE COPY FURNISHED TO DTIC CONTAINED A SIGNIFICANT NUMBER OF PAGES WHICH DO NOT REPRODUCE LEGIBLY.

SPACECRAFT MULTI-BEAM AND CONTOURED-BEAM ANTENNAS
by
P. Balling
TICRA
Kronprinsensgede 13
DK-1114 Copenhagen K
Danmark

SUMMARY

High-gain spacecreft antennas with multiple beams and contoured beams ara kay componants in satellite communicetions and direct broedcast systems. This is reflected on the latest genaration of communications setellites, where the entenna subsystem is the largest subeystem with its weight of mora than 300 kg. The entannas achieva e lerge communications capacity through multipla frequency re-uses and may be raconfigured to serve diffarent covarage araas.

The peper overviews the currant multi-beem and contoured-baam entanna technology. Different implemantations, reflector or lens with faad errey or direct redieting array, ere considered. Tha emphesis is placad upon systems with offeet paraboloidal reflectors. The limitetione of the offset reflector with respect to beam scanning end crose polarization ere reviewed. Computar-eided dasign procedures end dasign examplas ara presented.

1. INTRODUCTION

The antenne syetems cerried on boerd spacecreft have over the lest 25 yeers undergone e rapid evolution which parellels thet of the spececraft themselves. In fact, the spececraft system requirements have bean end continue to be a main driving force behind tha rejuvenetion of entanna thaory and technology which previously ware considerad to be mature disciplines. This evolution hae baan eupported by the eimulteneous edvent of ebundant computetionel fecilities.

Early spacecreft were emall, spin-stabilized setellites in low orbite. Tha antenne systeme wara simple, oftan with a low power in a nerrow frequency band, typically in the VHF band. Currant spacecraft hava become lerge end highly specielised end often carry severel antenna eysteme which ere teilored to the role of tha spacecreft. Most communicetions spececraft ere plecad elong the geoetetionary arc some 36,000 km above the surfece of the Eerth. The multi-beam and the contourad-baam antennes reviewed in thie papar ara axamplee of perticularly complex antenne syetems which significantly increase the cepacity end flexibility of theee aetellite eystams. By international agraament certein frequency bands heva bean allocatad for the different setellites servicae end rules heva been sat to minimiza the interferenca with othar satellite eyetems end with sarth-beeed systems [1]. Typically, the uplink signale from tha Eerth to the satellite end tha downlink signels back to the Eerth use different bande. Some of the most importent frequency-band allocetions for tha fixad satellite eervices (communicetions eetellitas) era indiceted in Teble 1. Tha frequency allocations differ elightly for three CCIR regions of the world and various rastrictions may epply so that the full bands cannot be used. Other bande era alloceted for communication with mobilu stations and for direct broadcast. Additionel bande ere alloceted at highar frequencies. Initially, the lower bands hava been the most popular as the technology has been better daveloped.

	Uplink	Downlink
C-band	5.925- 7.250 GHs	3.400- 4.200 and 4.500- 4.800 GHs
Ku-band	12.500-13.250 and 14.000-14.800 GHs	10.700-11.700 GHs
Ka-band	27.500-31.000 GHs	18.100-21.200 GHs

Table 1. CCIR allocations for tha fixad-satellite servica

1.1 Multi-Beam Antennas

Tha finita frequency spectrum available and the finite number of slots along tha geostationary arc for satellitas operating in the same frequency bend ara best utilisad by a multi-baam antenna which illuminates the covaraga area by a eumber of element beams. A hexagonal baam lattice is the most efficiant for contiguous area cuvarage. If the antenna radiates N beams and the available frequency spectrum is divided into K bands or channels so that adjacent baams usa diffarent bands, the frequency spectrum can be re-used M=N/K times. Figure 1 shows diffarent beam topologias whera the number in eech call or beam foot print gives tha channel number. The more channels the frequency band is divided into, the larger tha spacing will be between the calls where the same frequency is re-used and the better the isolation will be batween thesa beams. However, the number of times the frequency is re-usad will be lass. In practical systems, adjacent or overlapping beams may use orthogonal polarisations to improve the isolation or increase the number of frequenoy re-usea.

As an additional advantage of dividing the ooverage area into smaller celle, the spacecraft antenna gain is drastically increaeed. If all the power radiated by tha satellite were uniformly distributed over ±8.7° field-of-view eubtended by tha Earth, tho ultimately achievable gain would be 22.4 dBi. This would require an infinitely large, loseless antenna. In practice leee than 17 dBi ie obtained towerds the edge of the Earth using e horn antenna. With a multi-beam antenna, the upper limit on the achievable gain would ba eet by eise of the element-beam foot print or by the acceptable sise and complexity of the antenna systam and the accuracy with which tha aetenna can be kept pointed towards the coverage area. This shift

from ths early low-gain over medium-gain spacacraft antennas, which required huge earth-station antennas, to high-gein spacecraft antennas with small beam foot prints has in conjunction with improvements in satsllite power and low-noise receivsrs lead to the introduction of comparatively chsep, emall earth-station antennas. Mora aspects of multi-beam antennas are discussed in [2-4].

The simple beam topologiss of Figurs 1 carry some disadvantages. In real life, ths communications requirements are not uniformly distributed over the field-of-view and a multi-beam antenna system with many beams requires many transponders and a large switch matrix to provide the inter-connectivity between the uplink and the downlink beams. Also, it has not yet been practical without the usa of several antennas or excessivs antsnna losses to radiats element beams with the crossovar lavels down from the beam peak in the order of 3-4 dB needed for a contiguous coverage. These problems have laad to the concept of contoured-beam antsnnas whara sevsral of tha element beams are combined in a cluster or a composite beam.

1.2 Contoured-Beam Antsnnas

A contoured-beam antenne providss one or mora baams with foot prints on tha Earth tailored to speci-fic geographical areas. Sometimes thase antennas ara rsfsrrsd to as multi-beam antsnnas or shaped-beam antennas. Tha beam-contouring consarvas the satellita powsr and reducss the interferenca both with adja-cent frequency re-use covsraga arsas of tha same satellite system and with other systems. Figura 2 illu-strates the most common herdwere ussd to ganerata a contourad beam: a faad array which illuminates an offset paraboloidal reflector. Each fesd element, usually a small horn, generates a scanned pencil beam which is tsrmsd an slement bsam or a componsnt bsam. Tha foot prints of thasa slement beams on ths Earth ara indicated by small circlea on Figure 2. A contoursd beam which providas service to covsrage area A is obtained by adding the element beams radiatad towards tha coverage araa with appropriata (complex) wsight factors. Thase weights or faed excitations ars genarated by a beam-forming network (BFN) which often is a power divider traa with phase shifts providad by line langth differencas at the fead ports.

The fesd array and in particular tha BFN are tha most critical parts of a contourad-beam reflector antenna as they must realize the desired faed excitations with accaptable amplitude and phase tolerances and low VSWRs at both the feed ports and the baam port over the operating frequency bandwidth. The antenna system is raquirsd to operate in a hostile spacs anvironment with temparature axcursions in the ordar of -60 to 60 °C or more over the 7 to 10 year satsllite lifetima. The BFNs of most current contoursd-beam entannas consist of fixad power dividars and phase ahifters. These BFNs ara usuelly implemented in TEM-line in the 6/4 GHz bands and in waveguide in the 14/11 and 30/20 GHz bands. Waveguide BFNs have lowar insertion loss, but are haavier end more bulky than TEM-line BFNa. The stringent matching requiremants have laad to the elmost exclusive use of hybrid couplers rather than simple 3-port TEEs or E-plane couplers in tha power divider trea.

Advenced antenne systems includa on internetional communicetions aetallites switches to provida slow-ly reconfigurable beams to allow a satellite to oparete from differant locetions elong tha geostetionery arc and to accommodate traffic changes and on DSCS III fully raconfigurable BFNs with veriable ferrite power dividers. Future systems are likely to include mora variebla power dividers end varieble phese shifters in ferrite or solid-stete tachnology. This will allow both e high dagrae of beam flexibility and the fast reconfigurebility requirad for hopping and scanning beams with TDMA. Ultimately, BFNs ere expected to include many ective components to compensete for losses. This will provide vary compact and flaxible BFNs.

If ths antenna ayatem only is required to ganerate e single fixad contoursd baam, e shaped raflector illumineted by e single feed is en attrectiva solution with raspact to both performance end cost mainly becausa no BFN is required. This concept is reviewed in Section 5.

1.3 Choice of Reflactor, Lens or Arrey?

Tha use of a focusing device such e reflector or e lens provides e one-to-ona reletion between the element beams end the fsed horns. This rsletionship does not axist in the cese of en errey, where each errey element contributes to ell element beams, end en errey with several independent beams opereting at the sama frequency end polarizetion would suffer from significant lossas unless e Butler-matrix type BFN is used with orthogonal errey illuminetions for the different beams. In the ceses of multi-beam entennas where eech beam can be gensrated by s single fsed and of contoured-beams antennas where only e few element beams are used to ganerate the contoured beam, the BFN is much simpler for a reflector and a lens. As e result, array entennas have found only little use es spacecreft multi-beam end contoured-beam entennas. Nevsrthsless, ws will consider contoured-beam arrey antennas further in Section 7. A review of multi-beam erreys is given in [5].

The choice betwsen reflector end lens is more difficult. In the paet, most systems have used reflectors due to their low weight end cost, excellent bandwidth end polarisation properties and the fact that they can be enalyssd very accurately with ths existing RF enalysis methods. A main disedventage of the reflector is the need to use en offset-fed reflector geometry to avoid blockage by the large feed array, BFH and support structure. The offset-fed reflector has significently worse scan and oross-polsrisetion performance and occupies a larger volume on the spaceoreft than a similar center-fed reflector.

The lens is a focusing device with axial symmetry but without blockege. As furthermore the remaining dominant scan aberration, coma, may be removed by choosing the inner lens surface to be a sphere so that ths Abbé sins condition is fulfilled, lens antennas have considerable attraction for multi-beam applications [6]. Dielectric lenses are far too heavy for use et microwsve frequencies on s spacecraft, and new low-weight but slso more complicated lenses euch es the soned waveguide lens and the printed-oircuit bootlace or TEM-line lens outlined in Figure 3 have been devised. Thess lenses may be attractive in systems with somewhat less than 100 element beams where the number of waveguide or printed-circuit slements oan be kept reasonably small. Ths DSC3 III spacecraft in fact fliss three multi-beam soned waveguide lens antennas operating at about 8 GHz [4]. The bandwidth of a soned waveguide

lens is not competible with thoss steted in Tabls 1. The more broadbanded TEM-line lene hes been invsstigatsd for use at C band [7]. However, ite weight was considersd to ba so largs that the receivs and ths transmit function would have to be combined in one antenne. Tbe matching problem et the inner lene surfece could not be solved ovsr the combined frequsncy band and led to degradations of the element beams nsar tha axie. Becaues of their complexity and the still unsolved problems, lens entennas ere not considered further in this paper. It is expactsd that lens antennae will prove to be more useful at millimetsr and submillimeter wevelsngths.

Solid raflectors manufactur=d from carbon-fiber re-enforcsd plastic (CFRP) heve become very populer dus to their low wsight and excellent thermal behavior. Surfacs eccuraciee in the order of 1/100 wavelength RMS are requirsd to ensure low sidelobes. Solid offset reflectors providc excellent cross-polarization performance when ussd with circular polarization. Howsver, many domestic systems use linser polerizetion. This has led to the devslcpment of griddsd and duel gridded rsflectore to reduce tke cross polerization introduced by the offsst configuration.

2. FUNDAMENTALS OF CONTOURED-BEAM REFLECTOR ANTENNAS

2.1. Basic Definitione

Contoured-beam reflsctor antsnna eyetems hevs e unique sst of performance parametera. Most other entenna systems, including eerth stetion entennae, optimize the on-axie gain subject to certain eidelobe constreints oftsn definsd by en envelope. The driving eystem parameters are EIRP and G/T with sidelobe constreints edded to minimize interference. Cross-polarization requirements often only apply near the beam axis. Whsn en entenne is requirsd to ssrve an area rather than just e single direction, the minimum coverage area gain and not the peak gain becomee the eignificant parameter. Hence, tha etandard definition of antenna efficiency does not apply to contoured-beam antennas. Tha efficiency η of a contoured beam entenne is defined as the ratio of ths minimum coveregs erea gein MCAG to the gain G_{un} of e lossleae entenne which diatributes all the radiated power uniformly ecrose the specifisd coveraga arae Ω (in stsredians), i.e.,

$$\eta = MCAG/G_{un} \tag{1}$$

whers

$$G_{un} = 4\pi/\Omega. \tag{2}$$

Alternatively, the gein×area product, MCAG×Ω, may be defined. Due to the finite satellits pointing accurecy, the gain slope must be controlled within the area of uncerteinty for each earth station. Tha arae of uncertainty is celled the pointing-error box, aphere or ellipse dependent upon its actual shepa which is determinsd by ths setellite attitude control system. The coverage area Ω must includa the pointing error.

A pencil beam with a circular foot print is the simplest axample of a beam with an area coverage. If we essume e Geuseien beam shape and no losses, the power pattsrn

$$G(\theta) = 4 \ln10/\theta_{10} \ 10^{-(\theta/\theta_{10})^2} \tag{3}$$

givss the diractivity. Tha polar engle θ is measured from the beam axis and θ_{10} is helf tha 10-dB beamwidth. The minimum coverage aree gain occurs at tha edga of ths coveraga arse, $\theta = \theta_c$, and is maximizad for $\theta_{10} = \theta_c/\sqrt{\ln 10}$. This result also applies for Gaussian beams with elliptical foot prints. Thus, tha minimum coveraga erea gain is about 4.3 dB below paak gain for circular and alliptical foot prints. Tha associatad gein×area product is $4\pi \ 10^{-1/\ln10}$ or 15176 degraes^2, which corrasponds to e contourad-beam efficiency of only 36.8 per cent evan though that all lossaas heva been naglectad. This afficiency, which eccounts for the great gain differenca between tha idaal and tha practical global-coverage antenna in Section 1.1, may be improved by a flattar gain over the coverage aree and a staaper gein fall off at tha edge of tha covaraga araa.

Whan the antenna system providea multipla contourad beams, tha driving antenna paramatar becomas the isolation which can be echieved betwean beams which re-usa tha same frequency band aither through spatially separatad copolerizad beams or through orthogonally polarisad beams. Figure 4 illustretes tha diffarant definitions of intar-beam isolation which epply for racaive and transmit satellita antennea. Whan the satellita antenna transmits, an eerth station sarved by beam B may rscaive en interfaring signal via a sidelobe of beam A. Tha transmit isolation is defined as the ratio of the dasired signal from beam B to tha undesirad signal from beam A and depends on both the ralativa antenna gein and tha reletive transmit powar, i.e., thu ralativa EIRP. With tha setellite antenna raceiving, tha interferanca occurs via tha sidelobes of tha beam itself from earth stations outside the service eree. If all earth stetions trensmit with the same EIRP, the raceiva isolation is defined es the retio of the entenna gein towsrds tha earth stetion in the coverega aree to the antenna gein in the direction of the interfering earth stetion et the highast sidelobe level. The racaive isoletion is considered to be the m st difficult es e single highlavel sidelobe which falls in e frequency re-usa coverege, will destroy the isoletion on ell coverage-erae stations.

The minimum spacing between edjecent copolarised frequency re-usa coveregss, measured in beamwidths of the alemant beams, datarmines tha required epertura sise or resolutimn of the entenna system. An antenne pointing error of ϵ will reduce the minimum coversye area spacing by 2ϵ. Thus, e larga pointing arror may requira a significantly lerger end more complex antenna system.

2.2. Overview of the Current State-of-the-Art

The INTELSAT communicetione setellites provide en important example of the practical use of reflector antenna systems with multiple contoured beams. The complexity of in particular the C-band entenna systems have grown significent for eech new spacecreft eeries es illustreted by the increasing complexity of the coverages shown in Figure 5. INTELSAT IV A introduced two-fold frequency re-use through two spatially isoleted hemiephericel beams by meane of an array-fed offset pareboloidal reflector antenne system [8]. Thie concept wes further developed on INTELSAT V where four-fold frequency re-use was realized by the eddition of two smaller zone beams in the opposite sense of circuler polarizetion. These zone beams heve one shape when the epacecreft operetes over the Atlantic or the Pacific Ocean region and another over the Indian Ocean region [9, 10]. The trends towards both more frequency re-uses end more reconfigurability of the beam coverage contoure continue on INTELSAT VI. Two hemiephericel beams end four zone beams in opposite senees of circuler polarization provide eix frequency re-uses. The four zone beams ere reconfigured for eech of the three ocean regione providing a totel of 14 coverage beams with six ective in e given ocean region [11, 12]. The echievements and the limitations of this technology ere summarized in Table 2 [13]. It is common prectice to use separate antennas for the transmit end receive function to reduce both the bandwidth over which en entenne is required to operete end problems essocieted with passive intermoduletion.

The increesed number of frequency re-uses sets stringent sidelobe and cross-polarizetion requirements in the order of 27-30 dB over e field-of-view which extends epproximately ±10° from the subeetellite point to accommodate both entenna pointing errors and the epacecrart pitch biesing ueed to maximize the minimum spacing between spetielly ieoleted beams. As the spacecreft are pleced above the middle of the oceens, the beam coveregee fell near the maximum scen angle eo that ecen aberretions degrade the echieveble sidelobe isoletion. So fer, however, the diameter of the spacecreft entenne, meeeured in wevelengths, hae been moderete, end the number of beamwidths acenaed less then 6-7 half-power beamwidthe. This is demonstreted by the obeervetion thet for ell eetellites in the INTELSAT IVA, V to VI seriee the minimum eeparation between two copolerized coverages is about 1.5 element-beam beamwidths for 27 dB ieoletion [14]. Thie reletionship may continue for significently lerger reflector diameters if longer f/D ratioe or more complex feed erreys end BFNs cen be eccommodated to reduce the eberretions of the ecanned element beams. Figure 6 shows the celculated contoured-beam efficiency versue coverege eree size for INTELSAT VI. The two upper curves epply for a smaller feed element diameter of ebout 1.3 λ end in cese of the uppermost curve eleo the effect of e slightly increesed spacing between the coverege erees [15]. Other contoured-beam entennes elso for domestic/regionel end direct broedcest systems ere reviewed in [16-20].

2.3. Anelytic Model of Reflector Element Buams

A simple anelytic model is presented for the element beams redieted by emall circuler or squere feede in an offset pareboloidel reflector with circuler eperture. Effects due to the illuminetion teper end the spillover ere included to provide en eccurete essessment of the echieveble minimum coverege eree gein. The model neglects scen aberretions end cross-polerizetion end is therefore best suited for reesonebly lerge f/D retios end/or small scen engles. Even then we heve found thet the model may give surprisingly good predictions for the minimum coverege eree gein end the everege sidelobe level. The model cennot be used to determine the number of feeds or the feed excitetions eccurately. Therefore, the model is most useful in initiel trede-off studies to determine epproximately the entenna size end feed complexity given the coverege specificetions. The deteiled design optimizetion should be cerried out ueing element beams celculeted by en eccurete reflector entenne enelysis progrem such es GRASP [21].

Let the eperture distribution due to e single feed be epproximated by

$$g(\rho) = \alpha_o + (1-\alpha_o)[1-(r/e)^2]^n,$$

(4)

where the rediel veriable $\rho < e$. The parameter α_o is the reletive illuminetion et the reflector edge. Typicel parameter velues corresponding to en element beam would be $n = 1$ end $\alpha_o = 0.7$. We essume thet this amplitude distribution epplies for ell element beams. As we neglect scen eberretions, the phese distributions ceused by the leterel displacement of the feeds in the tilted focel plene only direct the weve fronts towerds the positions in the beam grid. The element beams are epproximated by the normalized patterns

$$f_j(\theta,\phi) = ke[\alpha A_1(kex_j) + \beta A_{n+1}(kex_j)].$$

(5)

The functions $A_n(x)$ ere given by Bessel functions $A_n(x) = 2^{n+1}(n+1)! J_{n+1}(x)/x^{n+1}$ so that $A_n(0) = 1$. The ergument depends on the perimeter ke of the circuler eperture in wevelengths end the distence

$$x_j = ((u-u_j)^2+(v-v_j)^2)^{1/2}$$

(6)

between the field direction (u,v) and the beam direction (u_j,v_j) in the uv-plane where $u = \sin\theta \cos\phi$ and $v = \sin\theta \sin\phi$. The angles θ and ϕ ere the poler end the esimuthal engle in e stenderd sphericel coordinete system directed elong the entenna boresight. The pattern parameters α end β in (5) depend via the edge taper α_o upon the primary parameters

$\Delta\theta_3$ - the helf-power element beam beamwidth, end
θ_B - the element beam spacing

es outlined below. In order to model the offset reflector and the feed element including spillover losses, the following secondary parameters

d_c/D - the reletive offset height or clearance,
d_e - the feed element spacing in wavelengths, and

θ_{10} - helf the 10-dB feed beamwidth

ere specified. Theee parameters are indicated on Figure 7. Given the above primary and secondery parameters, the parabole focel length f end the reflector diameter D can be derived. The reflector clearance d_c, the distance from the parebole exis to the reflector edge, should be so lerge thet no scanned baams are blocked by the feed array. The feed element spacing d_e and the feed beamwidth $2\theta_{10}$ ere roughly inversely proportionel for a given feed type.

Once the above parameters are given, en initial velues of the reflector diameter D, the focal length f and subtended semi engle θ^* ere calculated essuming a 3 dB edge teper by the epproximate formulae:

$$D = 1.029 \ (1 - 0.212 \ log_{10}\alpha_o)/\Delta\theta_3 \tag{7}$$

$$d_1 = (0.5 + d_c/D)D \tag{8}$$

$$f = (Kd_e/\theta_B + \sqrt{(Kd_e/\theta_B)^2 - d_1^2})/2 \tag{9}$$

$$\theta^* = Arctg \ d_1/f - Arctg \ d_c/2f \tag{10}$$

where K = 0.97. All angles are in rediens en all lengths in wevelengths. Note thet (9) hes no eolution if $\theta_B > Kd_e/d_1$. An improved velue may now be calculated for the everage aperture edge illumination using

$$\alpha_o = 10^{-(\theta^*/\theta_{10}^2)}/2/(1 + D^2/8(f^2+D^2)). \tag{11}$$

Given this velue, the values for D, d_1, f and θ^* ere updeted using (7) through (10). The offset paraboloid is now completely determined, end the pettern coefficients are determined from

$$\alpha = \alpha_o/N \ L_{so} \tag{12}$$

$$\beta = (1-\alpha_o)/[(1+n)N] \ L_{so}, \tag{13}$$

$$N = [(1+n+2n\alpha_o+2n^2\alpha_o^2)/(1+3n+2n^2)]^{1/2} \tag{14}$$

where

$$L_{so} = 1-10^{-(\theta^*/\theta_{10})^2} \tag{15}$$

gives the element-beam spillover lose. The pattern coefficients are normalised so thet the pattern (5) squared gives the directivity. This normalization is convenient for the normalizetion of the feed excitations discussed in Section 2.5. The effect of typicel element-beam edge tapere on the directivity is very emall, about 0.1 dB or less. The corresponding element-beam spillover loss ie more significant es discussed in Section 2.7. A number of other beem modele or simple dasign rules ara available for initiel contoured-beam reflector antenna trade-off end leyout [22, 23].

2.4 Array Elements

The erray element is a key element in detarmining the overell performance. The feed elemant must bs chosen in eccordance with the reflector geometry. For a apecified beam-spacing/beemwidth ratio, $\theta_B/\Delta\theta_3$, a smaller feed requires a shorter f/D ratio of the parabola than e larger feed. The $\theta_B/\Delta\theta_3$ ratio is usually close to unity correaponding to en element-beam croeeovar level of about -3 dB. Tha feed diamatars in the range from 1 to 1.6 λ match well f/D ratioe in the range from 0.7 to 1.4. For small f/D ratioe, the raflector subtended angle becomas largar and the spillovar losaes smallar. Howavar, tha scan lossae incraasee. The spillover losses era minimized if tha product $\theta_{10}d_e$ is kapt small. This parametar plays the role of ... array-element quality number and is raletivaly indapendant of tha size of a particular type of element es alreedy discussad in Section 2.3. For a small circular fundamental-moda horn the value of this parametar is about 1.00 while it is about 1.17 for a small dual-mode or Pottar horn. Small corrugatad horns are quite useless as array alemants beoause of tha larga spaca takan up by the corrugationa. From thasa oonsidarations it would appear that small fundamantal moda horn would ba the most useful for contoured-beam antenna applications. However, tha mutual coupling in tha erray anvironment will in practice annihilate the excellent theoratical performance of the small fundamental-moda radietor.

Tha circular wavaguide fead elements discussed above and tha square waveguide faed alements are used commonly in circularly polerised antenna systems. Many linearly polerized domestic/ragional systems uaa ractangular faeds of diffarent sises with or without dielectric loading often illuminating a dual gridded reflector. The faad horn dimensions ara optimized to match the image of tha coverage area in tha focal plane of the raflector. These systems may realise very raspeoteble values of the minimum coverage aree gain with a minimum of antenna hardwara but ere not dealt with in the paper [24, 25].

In e dual circulerly polerised antenna, e feed element in conventional waveguida technology consists of a horn rediator, a poleriser end en orthomode transducer. In a large antenna system with many feeds, this may be a very bulky and mechenically fragile system. Therefore, microstrip patch redietors hava racently receivad considereble ettention as a potantial very compact raplecemant .

2.5 Network Loss end Feed Excitation Normalisation

When . verel feeds ere excited simultaneously to genereta a contoured beam, the overell edge illumi-nation and spillover loss will in generel decrsase. On the other hand, the beam forming network (BFN) required to generate the optimised amplitude and phase distribution at the feed ports introduces Ohmic and mismatch losses. This BFN loss increases with the number of feeds ports as more layers of power dividers end longer line langths are required in the power divider tree. Fully reconfigurable BFNe may have signi-ficantly higher losses than fixed BFNe.

The feed excitatione e_j must be normalized by

$$P_{in} = 4\pi \sum_{j=1}^{N} |a_j|^2 = \begin{cases} 4\pi & \text{for directivity} \\ 4\pi 10^{-LBFN/10} & \text{for gein.} \end{cases} \tag{16}$$

Than, the directivity or the gein will be rafarred to the total incident powar et either the feed apertures or et the BFN input port. The directivity referred to the total redieted powar is derived if tha excitation normalizetion is

$$P_{rad} = 4\pi \sum_{i=1}^{N} \sum_{j=1}^{N} r_{ij} e_i a_j^* = 4\pi, \tag{17}$$

where r_{ij} is the normalized mutuel resistance end $r_{ii} = 1$.

2.6. Mutual Coupling

For a sufficiently lerge array element with e Geussien pattern, the normalized mutuel resietance is

$$r_{12} = e^{-(kd_{12}\theta_{10})^2/4\ln 10}. \tag{18}$$

Thie indicetee that tha mutual rasistance depends with the approximatione made only on the product $d_{12}\theta_{10}$, which for edjacent faade is equal to tha feed quelity number. Thus, the requirements for low mutual coupling and for a small spillovar loee ere in conflict: A large value of $d_a\theta_{10}$ reduces the mutuel coupling but increeees the element beam spillovar loss. In e study of feed-arrey directivity, $\cos^q\theta$-epproximatione to the feed elemant pattern heve been used [26].

The mutuel resistance given by (18) is der$\_\_$d from an idealized feed pattern end neglects highar-order modas and crose polarization. It relatas to the small signal which appeers at the port of e feed when an edjacent feed is excited. Thia effect is quite negligible for precticel feed-errary elements and (16) is a good approximation to the power radiat$\_$d by the feed arrey. Howevar, the affect of the array environment on tha element pattarn is much etronger. This effect, which may be termed mutual ecettering, eets up tha crose-polar mode end higher-order mod$\_$e et the radiating eperture and hae a pronounced effect on the crose-polar parformanca.

Much work hee bean carried out on mutual coupling in phasad-errey antenna syetems using tha concept of tha active element pattarn and tha unit call approach. Thasa techniques do not apply to contourad-beem antanna feed errays which heva very non-uniform amplitude and phase dietributions. The number of elemante ie typicelly smaller than in e pheeed array and the element eise is larger. No electronic ecenning takas place end tha blindness affecte of ecanning phaeed arraye ara of no concarn. The concept of the embedded element pattern is mora ueaful. Tha embeddad feed pattern is defined as the pattern tha faad rediates in the array anvironment with tha feed element excitad end all othar alemante terminatad with their actual loads. Miematches at the fead ports into the BFN heve been noted to hava a significant effect on tha cross polarizetion - in particular for circular polarization.

A comprahansive study of mutual coupling in contoured-beam antenna faad arreys has bean raported in [27]. The method of momente ie usad and the results epply to a finite number of circuler wevaguide feeds in e ground plane.

2.7. Spillover Loee Calculation

The spillover loss of e contourad beam will be lowar then that of an element beam bacausa of tha array fector. The epillover loee ie definad ae tha ratio of the feed power which hit the raflactor to the total radieted feed power. The total power redieted by the faad erray hae been celculeted (16). The element beams overlap end era usually not orthogonel. Therefora, tha power intarceptad end radiatad by the reflactor must be datarmined by intagreting the total raflector far fiald. It is much eimpler, howevar, to determine the power rediated by the reflector by integrating tha Poynting vector ecroes tha raflector eperture A es propoeed in [28]. We than obrein for tha amplitude dietribution in (4)

$$P_{rfl} = 4\pi \sum_{i=1}^{N} \sum_{j=1}^{N} a_i a_j^* \left[\alpha^2 A_1(kax_{ij}) + 2\pi\beta A_{n+1}(kax_{ij})\right.$$
$$\left. +(n+1)^2 \beta^2 A_{2n+1}(kax_{ij})/(2n+1)\right], \tag{19}$$

where the pattarn coefficients α end β ere defined ebova. Tha parameter x_{ij}, eimiler to (6), ie the epacing between the beam centere in the uv-plene. The "crose corraletion" pattern in (19) ie wider than the elemant-beam pattern axcept in tha cese of uniform illumination. If the element-beam positions coincide with tha nulls of the "crose-correletion" pattern, tha beams decouple and becoma orthogonal. It eppear that "loeees" due to non-orthogonel beams ere of e fundamentel netura end may be releted to different mechanisms in different antenne eyetems, e.g., BFN loeee, epillover losses in reflector and lens eyetems and greting-lobe loeees in srraye [29].

Figure 8 ehowe tha epillover loeeae for e eingla element beam and a clueter of eeven elemant beams. The feed epacing is kept constant equal to 1.07 λ and the beam spacing ie increeeed by decreasing the focal length. The engle subtended by the reflector inoreaeee with increaeing beam epacing, and the element beam spillover lose decreeeee. The dotted curve is the element beam epillover lose oslculeted eccurately by a reflector antenna analysie program. The spillover loss of the 7-element cluster ie much lower than that of the element beam and elmoet independent of the beam spaoing. For e fixed reflector geometry, the beam epacing (or the beam crossover level) may be veried by changing tha feed epacing. Table 3 givee the epproximate spillover losses of both eingle and uniformly excited 7-element olusters of oirculer fundamental-mode and dual-mode feeds. The table gives the calculeted spillover losees for $\theta_B/\Delta\theta_3$ equal to 0.7, 1 and 1.3 correeponding to crossover levels of 1.5, 3, and 5 dm.

	Single feed			Cluster		
$\theta_B/\Delta\theta_3$	0.7	1.0	1.3	0.7	1.0	1.3
TE_{11}	5.7	3.1	-	1.5	1.3	-
$TE_{11}+TM_{11}$	6.8	4.1	2.3	2.6	2.4	2.1

Table 3. Spillover loss in dB.

A significant fraction of the large element-beam spillover for small beam spacings may bs recovered by the array factor. For the dual-mode feed cluster, where tha greting lobe losses are larger dus to the larger feed size, the effect of the array factor on the spillover loss becomes vary small for large beam spacings. A hexagonal array lattice will reduce the grating-lobe losses. For each feed type, a smaller feed spacing will slightly reduce the cluster spillover loss. Ths table indicates that there is a need for improved feed alements which utilize the focal-plane area more efficiently but without high mutual coupling. Another end probably more promising remedy might be to use improved reflector systems.

Even though the spillover loss of a contoured beam cen be considerably reduced by the array factor, it can not be neglected. In the sensa that this loss represents radiated power, it is very harmful in a frequency re-usa antenna system if it is intercepted by ths antenna or by other satellite structures end re-radiated as cross polerization back into the coverage or as high sidelobes into adjacent coverages. Such antenna-farm effects are difficult to predict as they depend upon ths wide-angle radiation from the feed array end require special analysis software.

2.8. Scan Characteristics of Single Reflectors

Figure 9 shows isogain contours for the on-axis end some scanned elemsnt beams for a 3.2 m offset paraboloidal reflector at 4 GHz with en f/D ratio of 1.3. As a beam is scanned a way frcm boresight, a gain loss end a beam widening occur. Theee beam degradations depend for a given scan angle upon the D/λ ratio, the offset angle θ_o, the f/D ratio, end the aperture illumination. For the single offset paraboloidal reflector, whars the scan degredation is due to astigmetism [30], the scan loss in dB for the scan angle θ_{sc} may be approximated by

$$L_{sc} = C(n,\alpha_o) \ (D/\lambda \ D/f \ \sin\theta_o \ \sin\theta_{sc})^2, \tag{20}$$

with $C(n,\alpha) = 0.1116\left[(n+1)\alpha+6(1-\alpha)/(n+2)(n+3)\right]/(1+n\alpha)$. The parameters n end α_o are tha axponent end the edge taper of the reflector aperture illumination (4). For scan losses larger than 5 dB, (20) predicts too large losses. The scan loss is not a loss in radiated power as the BFN loss end tha spillover loss. It represents a loss in tha resolution or the beam-contouring capability of the reflector due to the widening of the element beams for large scan angles. Some scan degradation may be compensated for by a more complex feed array.

The scan losses of the center-fed paraboloidal reflector are for tha same aperture diameter, f/D retio, scan engle end aperture illumination order of magnitude less then those of the offset-fed reflector. The dominant aberration is due to coma, which has a minor impact on scan loss end mainly degrades the sidelobe performance [31]. As the total scan loss is determined by a combination of coma, higher-order estigmatism end spherical aberration, no simple expreseion exists for ths scan loss in the canter-fed paraboloidal reflector.

2.9. Polarization Considerations

Circular polarisation was initially chosen for use in the international communications satellite system because of the Faraday rotation. When a linearly polarised signal traverses the ionosphere, the polarisation plane undergoes a rotation. At 4 end 6 GHz, the maximum Feraday rotation is approximately 9 and 4° with opposite directions for transmit end receive (CCIR Report 551-1, Sect. 2.3.1). This choice of polarisation wes fortunate from the point-of-view of antenna technology. Circularly polarised offset reflectors do not generate cross polarisation but exhibit a slight beam squint in the plane perpendicular to the plane of symmetry [32, 33]. Ths magnitude of this beam squint is given by the approximate formula

$$\Delta\beta = Arcsin(\lambda\sin\theta_o/4\pi f). \tag{21}$$

The direction of the beam movement depends upon the hand of the polarisation. The Feraday rotation is inversely proportional to the square of the frequency end presents no problem above 10 GHz. Then, depolarisation caused by rain becomes important end from the point-of-view of cross polarisation, circular polarisation becomes the worst possible choice. The shape of rein drops is generally spherical. However, the shape of falling rein drops becomes slightly elliptical due to the air resistance. The rein-induced attenuation end phese shift are maximum (minimum) for the polarisation aligned with the major (minor) axis of the rein drop. No depolarisation takes place for linear polarisation aligned with the major or the minor axis of the rein drop. In practice, the depolarisation is minimised for linear polarisation aligned with local earth station vertical end horisontal (CCIR Report 564-2, Sect. 8.2). Thus for frequency re-use antenna systems in the 14/11 GHz bands end possibly even the 30/20 GHz bands, linear polarisation should he used aligned with the average local verticel end horisontal within each coverage area [34]. However, this alignment will reduce the cross-poler isolation between adjacent coverage areas under clear-sky conditions as the polarizations then no longer are orthogonal.

In the single offset paraboloidal reflector, the feed axis is in general tilted to bisect the angle subtended at the focal point by the reflector in its plane of symmetry. This feed axis tilt generates two cross-poler lobes in a linearly polerised system [32, 35, 36]. The peak of the cross-poler lobes occurs in the plane perpendicular to the plane of symmetry. For a uniformly illuminated aperture, the peak cross-polar level relatively the peak copolar level is

$$E_{cross}/E_{co} = 0.36 \ \theta^* \ \tan\theta_o/2, \tag{22}$$

where θ^* (in rediens) ie the eemi angle eubtended by the reflector. A tapered eperture illumination will decreeee the cross polarieation elightly. Any eignificant reduction requiree either a more complicated feed element, e more complex feed errey design, or that e gridded reflector be used.

3 OPTIMIZATION OF CONTOURED-BEAM REFLECTOR ANTENNA SYSTEMS WITH FEED ARRAYS

The syntheeie of a contoured-beam entenne eyetem may be divided into etepe. Initielly the fundamental antenna performance requiremente euch ee

- coverage erea(e),
- minimum coverage-aree gein,
- maximum coverege-area gain elope,
- eidelobe and oross-poler ieolation end
- frequency band

muet be epecified. Next, the antenna deeigner may identify the range of e number of antenna parametere euch ee

- reflector eperture eiee, and
- feed-errey complexity

and examine the performance trade-offe vereue the antenne eyetem eiee and complexity. Theee trade-off etudiee require thet optimum feed excitatione be determined and the reeu:ting con+oured beame be enalyzed for eeverel entenna configurations. If theee etudiee ere cerried out with eimple enalytic element-beam modele, lerge eavinge can be reelieed in both humen effort and computer time.

When e viable eolution hae been identified by theee initial optimizatione, an element-beam leyout with half-power element beam beamwidth $\Delta\theta_3$ end the element beam epacing θ_B will be known. Given this element-beam grid, the feed-element eiee end the orientation of antenne on the eetellite, an initiel reflector entenna end feed array layout may be determined anruring thet no blockage occure. Then, the detailed optimizetione ere cerried out ueing element-beam date decermined by an accurate reflector entenna enelyeie program. It ie deeirable to include ae meny potantial error eourcee ae poeeible. Degrading effeote not predicted by the eoftwere can be included by meane of meaeured data, e.g., of the patterne of the feeds embedded in the array. In case the reeulte of the optimieatione indicete that the performance requiremente can not be met, theee requiremente or the range of antenne paiametere being coneidered must be revised.

3.1 Optimieation Proceduree

Many different, more or leee rigorouely baeed optimieation proceduree have been propoeed to determine the feed exoitatione which provide the "best" contoured beam. It appeare that no optimieation procedure ie complete. Ueually tha antenna designer epecifiee the reflector and the feed arrey geometry. Only then an optimization procedure determinee the "best" feed excitatione by optimieation of the antenna performance, e.g., gain and ieolation, over a finite number of pattern sample po:nte. Theee eample pointe will be termed eyntheeis etatione ee they may not correspond to actual earth etatione. A more complete optimieetion cen be carried out by repeating the feed exoitation optimieetion for a large number of antenne geometriee. A generel optimi;ation procedure may optimiee both element-beam grid end excitatione but the ueefulneee of the reeulte will be limited by the eccuracy of the element-beam model. For prectical entenna syetema, it ie etill prohibitive and probably not deeireble to include in the oloeed optimieation loop a complete electromagnetic analyeie Jith a.o. BFN toleranoe analyeis and feed-array mutual coupling enalyeie.

A contoured-beam syntheeie ie a power-pattern eyntheeis problem as opposed to a field-pattern eyntheeie problem. Furthermore, the power pattern are only epecified in certain regione. The power pattern in the complementary regione of the far-field epheie and the phaee pattern ehould be allowed to float in the optimieation end take on eny values which improve the power pattern in the regione of intereet. Thue, even the apparently eimple problem of determining the beit feec excitatione for e specified antenna geometry ie e complex nonlinear problem and it can not be determined if a eolution ie a locel or a global optimum. It appeare often, however, that the optimum ie quite flet ec that emall changee in antenna geometry, initial feed excitation input to the optimieation procedure, stations locatione, etc. may reeult in quite differant feed excitatione but very often only in emall changee of the antenna performance. It is recommended to input different initial eolutione to iterstive optimization elgorithms and to oarry out eensitivity etudiee of the final eolution with reepect to axcitation errore. The optimiaation ie in generel carried out on the copolar field only. In systema which implement frequency re-uee by meane of orthogonal polarizatione, the required croee-polar performance is typically implemented by antenna designe which have low inherent croee polarization.

The following four eectione deecribe a least-equaree optimization procedure with a power conatraint, the formulation of the minmax eyntheeie problem, e minmax optimization procedure which utilisee e generel-purpose algorithm which recently has been extended to work more efficiently on contoured-beam eynthesis problems, and recent progreee with minmax or maxmin algorithme which have been developed epecifically for contoured-beam reflector antenna synthesis. Many different approaches are described in the litereture [e.g., 37-45].

3.2 Leaet-equaree Syntheeis

The method, eleo known as the regulariestion method, ie explained below using e matrix notation [46]. We define the matrix $e = (e_{ij})_{MxN}$ where e_{ij} is the contribution of element beam j, $j = 1,2,...,N$, towarde synthesis etation i, $i = 1,2,...,M$. Two column vectore $s = (a_j)$ and $g = (g_i)$ contaia the N excitatione and the deeired field on the M synthesis etatione. The number of Synthesis stations exceeds in generel the

number of element beams and a solution can only be found in a least-squares sense. In order to optimize the minimum coverage area gain, the power input to the antenna must be constrained. Therefore we add the norm of the excitation vector e, which gives the incident power (16), to the least-squares pattern error by a Lagrange multiplier α. The expression to be minimised is then

$$J = (e^T e^T - g^T)W(ea - g) + \alpha e^T e, \tag{22}$$

where the weight matrix W is a diagonal matrix and the superscript "T" denotes conjugate transposition. This gives the following matrix equation for the unknown excitations e

$$(e^T We + \alpha)e = e^T Wg. \tag{23}$$

Initially, we only specify the amplitude of the desired field on the synthesis station by

$$g_i = (G_o p_i f_{oi})^{1/2}, \tag{24}$$

where G_o is a gain normalisation constant, p_i the desired relative gain level, and f_{oi} a path length correction factor if flux density rather than gain shall be optimized. As gain normalisation constant we can use the peak achievable minimum coverage area gain (1) with a back off. This requires that the angular area Q of the coverage area be determined.

The relationship between the Lagrange multiplier α and the incident power is established by means of the eigenvalue equation corresponding to (23). The matrix $e^T We$ is Hermitian and the positive real eigenvalues and the eigenvectors may be determined by standard techniques. We expand the unknown excitation vector in the complete basis formed by the eigenvectors. The expansion coefficients are determined in terms of the Lagrange multiplier α which in turn is derived from the power constraint (16).

The specification of the desired field (24) implied a constant pattern phase. To remove this limitation in a heuristic way we include a phase factor $\exp(j\Phi_i^k)$ which is updated iteratively. At the kth step we determine the pattern phase from the excitations derived in the k-1th step by

$$\exp(j\Phi_i^k) = \sum_{j=1}^{N} e_j^{k-1} e_{ij} / \left| \sum_{j=1}^{N} e_j^{k-1} e_{ij} \right|. \tag{25}$$

A new right-hand side of (23) is calculated and a new value of α must be determined for each step in the phase iteration. However, the eigenvalues and the eigenvectors remain the same throughout the iteration. The iteration is terminated when the relative change of the least-squares error (22) decreases to a specified value.

3.3 Formulation of Minmax Synthesis Problem

The least-squares solution discussed above will in many cases be very good except, possibly, on a few critical synthesis stations. A minmax method may improve the performance on the these critical stations generally at the expense of the average performance over all stations. The minmax optimisation problem consists of finding the feed excitations e_j so that the realised power gain

$$pw_i = \left| \sum_{j=1}^{N} a_j e_{spj} \right|^2 \tag{26}$$

minimizes the maximum value of the residual or pattern error

$$f_i = w_i \left| pw_i / (f_{os} G_o) - p_i \right| \tag{27}$$

over all pattern constraints i, i.e., synthesis stations s and polarisations components p. In (26) and (27), the following notation has been used

e_{spj} field towards station s in polarisation p from element beam j,
f_{os} path length compensation factor towards station s if flux density is optimised,
p polarisation selector equal to 1 or 2,
p_i desired relative power level for pattern constraint i. Often $p_i = 1$ for coverage-area constraints, $p_i = 0$ for isolation constraints and p_i equal to a specified gain roll-off function with a back off if a reference pattern shall be enforced,
s synthesis station number, $s = 1,2,\ldots,M_s$, and
w_i weight factor used to equalise coverage and isolation constraints.

The residuals for coverage area pattern constraints which exceed the gain goal are set equal to zero.

The minmax optimisation problem consists of determining the feed excitation vector e which minimizes the maximum residual

$$f_{minmax} = \max_i f_i. \tag{28}$$

The corresponding least-squares error (22) minimises the average deviation over all stations. The weight factors w_i and W_i are used to increase the magnitude of the residuals in isolation areas to correspond to the magnitude of the copolar residuals in the service area. If the minimum coverage area gain is MCAG, the maximum sidelobe (cross-poler) level is MSL and the coverage area weight is unity, the minmax sidelobe (cross-poler) weight factor

$$w = (G_o - MCAG)/MSL \tag{29}$$

will equalise the residuals. The weight factors behave slightly differently in the minmax and in the least-squares optimisation. The best agreement between the two optimisations is obtained if $W_i = w_i^{1/2}$.

3.4 Synthesis by General Minmax Algorithm

The general minmax algorithm is an extension of the iterative method described in $[47]$. Let the column vector x_k represent the excitation vector et the kth etap of the iteration, $f_i(x_k)$ the associated error or residual (27) et the ith pattern constraint, the column vector b_{ik} en approximation to tha gradient of tha residual with respect to the excitations and the column vector h an increment to tha excitation vector. Then,

$$F_k(h) = \max_i \ (f_i(x_k)+b_{ik}^Th) \tag{30}$$

ie e linear epproximation of the minmax pattern error (28) for small values of $|\ h\ | = \max|hj|$. At each etap of the itaretion, tha linear subproblem (30) is solved by linear programming subject to a bound on the solution,$|\ h\ |< \lambda_k$, giving tha solution h_k. The vector x_k+h_k is accepted es the new approximate solution if the non-linear objective function has decreased. Otherwise the etep is rejected and repeated with e smaller λ_k. The bound λ_k raflects the region near x_k where (30) is a reasonable approximation to the original non-linear problem and it is adjusted automatically during the iteration. Tha approximations to tha gradients are updated using e rank-one formula by Broyden $[48]$,

$$b_{ik+1} = b_{ik}+(f_i(x_k+h_k)-b_{ik}^Th_k)/(h_k^Th_k)h_k. \tag{31}$$

In e contoured-beam optimization, the number of synthesis atations cen be large in particular when a global envelope constraint in anforced ae in Section 4.2 or when several contoured beams with common excitations are optimized simultaneously ae in Section 4.3. A significant amount of storage is needed for the derivative matrix and large linear programming problems must be solved at each atap of the iteration. In practical problems, however, the number of stations where the pattern error (residual) ettains the maximum value is small compared to the total number of stations. Tharefore at each etep, we identify the stations within a specified range of the largest residual. These stations define the overall pattern error F in e neighborhood about x_k and ere called the active stations. Working mainly only with the stations within e range of the largest residual, we realize large savings in storage and computing time wheress tha convergence properties remain the same. The derivative matrix is stored end updated only for the active stations - typically about 1/5 and less of ell stations. The sise of tha linear programming sub problems era reduced by the same proportion. However, ell stations are still checked et each etap of the iteration and tha active set is updated as required. The gradients of tha rasiduals which are active et both x_k and x_k+h_k are updated by (31). For the newcomers we use e difference epproximation since we have no estimate b_{ik} of the gradient et x_k.

In case of e singular problem, the iteration may become slow because the process is caught in e long valley with steep sides $[49]$. It is e characteristic of e singular problem that with N excitation variables, the number of worst stations where the residuals are equal to tha maximum residual will be lass than N+1. The number of worst stations is generally considerably lass than the number of ective stations used in tha iteration and less than tha number of excitation variables even in the final stages of the iteration. Thus, most contoured-beam synthesis problems appear to be singular. When we decide that the process hes been ceught, we apply e "special" non-descent iteration to bring the process out of tha valley. It can be proven that tha extended method theoretically has tha same convergence properties es its precessor whereas in practice the new method is considerably faster and cen handle much bigger problems within the same computer memory.

3.5 Specialised Minmax Algorithms

The general minmax algorithm provides tha maximum degree of freedom in the design. We may choose to optimise only the amplitudes, only the phases or both the amplitudes and the phases of tha excitations with only small changes of the software. Also, the location of tha element beams may be optimised or degrading affects such es BFN frequency dispersion and BFN random errors could be accounted for. However, the general algorithm does not take advantage of the special properties of e specific contoured-beam synthesis problem as opposed to, e.g., microwave network synthesis problems. The general algorithm does not use the closed-form analytic derivative of residuals which ere available in special cases but uses approximations derived by finite differences and Broyden's formula. These epproximations ere both more time consuming and more inaccurate. They may result in a reduced rate of convergence in the final stages of the iteration, where a large linear programming problem may have to be solved at each atep.

A simple minmax algorithm hes been proposed by in $[50]$ to be applied in cases with amplitude only or both amplitude and phase excitation optimisation. For the excitation normalisation (16) with no loss, the derivative of the ith residual f_i (27) with respect to a_j is given by

$$f_i'{}_j = 2\Big[\big(\textstyle\sum_{j=1}^{N}a_{ij}e_j\big)a_{ij}^* - \big|\textstyle\sum_{j=1}^{N}a_{ij}e_j\big|^2e_j\Big]. \tag{32}$$

The factor $w_i/(f_{oi}G_o)$ hes been suppressed. It is further shown in $[50]$ thet the gradients ∇f_i are perpendicular to the excitation vector. At each etep in the iteration, the active stations ere identified and e best search direction is found by solution of a system of linear equations. The length of the incremental vector Δa_k to be added to the excitation vector a_k in tha kth etap is determined very efficiently by e linear search.

We found that each etep in the iteration proceeds extremely fast compared to the general minmax algorithm and that very often good results are obtained. The range of the residuals which define the active stations gradually decreases during the iteration. In our implementation, the method sometimes requires very many iterations to terminate. When the number of active stations becomes equal to the number of excitations, tha linear system of equations used to determine the search direction becomes singular and the iteration is forced to terminate.

Recently, the convergence of the method hes been considerably improved by determining the best search direction by solving a linear programming problem and improving the linear search $[51]$. Only the worst stations are considered in the search direction determination. The results indicate that order-of-magnitude saving in computer time may be realized when closed-form derivatives are used instead of

derivetive epproximations. A possible future extension may be to implement e hybrid algorithm which would use enelytic derivetives whenever they ere eveileble end derivative epproximations otherwise.

4   SYNTHESIS EXAMPLES

The optimisetion procedures described in Section 3 have been implemented in a eynthesis software. This section gives three examples of results obteined with this softwere peckege. Other recent design examples includes dual-mode entenne optimisetion [52] and en offset side-fed Cassegrein entenne with ten contoured beams [53].

4.1   Antenne without Stringant Sidelobe Specificetions

4.1.1   Contoured-beam entenne specificetions

The optimizetion of e contoured-beam reflector antenne system for e European Communicetions Setellite coverege ie provided to illustrete the design procedure. The entenne is e trensmit entenne with the requirements outlined below:

Frequency band:	10.7-11.7 GHe
Polerisetion:	RHCP
Min. coverege area gein including	
BFN loss and spillover:	28 dBi
Max. pattern slope in coverege erea:	5 dB/degree
Max. copolar sidelobe level:	-20 dB
Min. cross-poler isoletion in coverege eree:	30 dB

An erea coverege including e 0.2° pointing srror wes specified. The number of feeds ves anticipated to be between 20 and 30 and the antenna envelope should be compatible with the ECS pletform end the Arlene leuncher. The feed element wes chosen to be e small conicel horn pleced in e hexegonel grid with en element spacing of 1.07 λ et the center frequency. The coverege wes composed of four isoleted stetions end e lerge erea specified by e piece-wise linear contour. The eree specificetion wes converted into discrete stetion specificetions by edding synthesis stetions inside the piece-wise linear contour. It wes found that e spacing between the samples in the uv-plene of

$$\delta_{uv} = 0.01 \, \Delta\theta_3, \tag{33}$$

with the element beem beamwidth $\Delta\theta_3$ in degrees, geve e reesonsble trede off between eccurecy end computation time. This corresponds to ebout 60 per cent of the maximum Nyquist sempling spacing λ/D end ellows for truncation effects near the edge of the coverege, the tilt of the effective aperture plene elony the plene of the reflector rim curve, etc. When e lerge renge of element beam beamwidths is being considered, it becomes necessery to use more than one coverege sampling spacing. Figure 10 shows the 58 synthesis stetions representing the ECS coverege for the half-power beamwidths 2° end 1.5°. The spacing (33) between the internal samples is 0.015 corresponding to 0.86°. For the half-power beamwidth equel to 1.2°, the sample spacing wes reduced to 0.012 or 0.69°, and 81 synthesis stetions were obteined.

4.1.2   Initial optimisetion with enelytic element beems

The preliminary design trede-off was cerried out with the enalytic beam model for the beamwidths $\Delta\theta_3 = 2.0^\circ$, 1.5° end 1.2° to determine approximately the reflector sise end the number of feed element. In each cese, the beam spacings $\theta_B = 1.2$, 1.1 and 1.0 $\Delta\theta_3$ were considered. The initiel beam grids set up included all element beams with e distance less than Δ_{BS} from the neerest stetions. With $\Delta_{BS} = 1.25$, 1.00 end 0.80 θ_B, e total of 27 initiel beam grids were considered. In each cese, the flux densities on the Eerth were optimised teking into eccount the path length differences between the setellite end the synthesis stetions. An initiel set of real excitations was obteined by the least-squares algorithm end used es starting point for the minmax algorithm which elso veried the entenna pointing end the beam lettice orientetion and spacing. All the excitetions ere real-valued beceuse the element beams are real-velued.

The configuration with $\Delta\theta_3 = 1.5^\circ$, $\Delta_{BS} = 1.65^\circ$ and initial velue $\theta_B = 1.65^\circ$ was found to give the best compromise between antenne complexity and performence. However, the optimum is quite flet. Figure 11 shows optimised the element-beam ley-out, which includes 24 element beams, end the isogein contours of theoptimised contoured beam 1, 2, 3, 5, 10, 15, 20, 25, and 30 dB below peak gein. The number of "ective" stetions in the minmax optimisation is 17, which is well below 24, the number of element beams. Thin indicetes thet we are dealing with e singuler problem. Only four least-squares residuals exceeded the minmax residual. The essocieted synthesis stetions belonged to the set of "ective" stetions in the minmax solution. The analytic beam model provides an initial entenne geometry shown in Figure 12 ee seen from the dish. The feed ley-out is the imege of the element-beam ley-out in Figure 11.

4.1.3   Finel optimisetion with PO/GTD element beems

The initial antenna geometry was further optimised using accurste element beam data determined by PO, GTD and Whittaker reconstruction. These beams are complex-valued so that both feed excitation emplitudes and phases were optimized. The initial least-squares feed excitations were determined using iterstive updating of the pettern phase and used as starting point for the minmax excitation optimisation. The optimised excitations were inspected for weekly excited feeds. These feed were eliminated and the excitations of the remaining feeds re-optimised. Table 4 summarises the principal results with en essumed BFN loss of 1.4 dB.

	Least-square Min flux	Min flux	Minmax Min gain	Spillover
Analytic beam model:				
all 24 beams	27.85	28.31	28.09	-1.02
PO/GTD beams from GRASP:				
all 24 beams	28.21	28.40	28.17	-1.21
-beams 18, 20 and 22	27.81	27.97	27.73	
-beams 20 and 22	28.15	28.26	28.02	

Table 4. Results of ECS optimizations. Levels in dB and dBi.

Several observations may be made. Firstly, the least-square solution is in all cases quite good compared to the much more time consuming minmax solution. Secondly, the prediction obtained by analytic element-beam model is very close to the one obtained using a much more accurate element-beam model. The element-beam model is quite sensitive to the value assumed for the feed quality number $d_e g_{10}$. Thirdly, deleting feed or element beam 18 has a significant impact on the solution so that caution should be exercised when feeds are eliminated. The optimization should begin with a generous number of feeds which gradually are removed. Each time, the excitations of the remaining feeds must be re-optimized. Figure 13 and 14 show the element beam half-power contours and the contoured-beam isogain curves derived by means of PO, GTD and Whittaker reconstruction at 10.7 and 11.7 GHz. The decrease of element-beam half-power beamwidth with increasing frequency may be noted. The agreement with the analytic beam model in Figure 11 is good except for a slight widening of the low level contours in Figure 13 and 14 due to the scan aberrations neglected in the analytic element beam model.

The finite tolerances of the BFN, mismatches, frequency dispersion in the BFN and mutual coupling will cause the realized feed excitations to deviate from the optimum values determined by the synthesis software. Excitation errors not accounted for will degrade the antenna performance. Some of the degrading effects may be included in the pattern optimization. Thus, it has become common practice to carry out the excitation optimization simultaneously at both edges of the frequency band if the antenna is required to operate over any significant bandwidth. Table 5 summarizes the results of computer simulations of the effect of random excitation errors on the minimum coverage area gain. For the range of errors and the configuration considered, amplitude errors seem to be more serious than phase errors. For practical applications, the average excitation error should be less than a few tenth of a dB in amplitude and 5° in phase.

Peak excitation		Gain degradation due to		
amplitude error	phase error	amplitude only	phase only	amplitude and phase
0.3 dB	3°	0.19 dB	0.00 dB	0.17 dB
0.6 dB	6°	0.32 dB	0.09 dB	0.44 dB
0.9 dB	9°	0.61 dB	0.16 dB	0.66 dB
1.2 dB	12°	1.16 dB	0.24 dB	0.88 dB
1.5 dB	15°	1.12 dB	0.32 dB	-

Table 5. Degradation of the minimum coverage area gain as a function of random excitation amplitude and phase errors.

4.1.4 Measurements on array-fed contoured-beam antenna

In the European Space Agency's COBRA (contoured-beam reflector antenna) program, the prototype of the antenna described above was designed, manufactured, integrated and tested [54]. The rms deviation of the measured amplitude and phase excitations from the nominal values are indicated in Table 6 at the edges and the center of the frequency band.

Frequency	Amplitude	Phase
10.7 GHz	0.58 dB	5.6°
11.2 GHz	0.24 dB	5.9°
11.7 GHz	0.59 dB	6.5°

Table 6. Rms deviations of excitations at feed ports.

Figure 15 shows in full line the measured copolar contours 1, 3, 5, 10, 15 and 20 dB below peak gain at the edges and the center of the frequency band. The calculated contours 3 and 20 dB below peak gain are superimposed in dotted line. The agreement is fair apart from 11.7 GHz where strong mutual coupling effects between the small circularly polarised feeds not accounted for in the analysis are believed to degrade the minimum coverage area gain from 28.1 to 25.6 dBi at Barcelone. The cross-polar discrimination was better than 28 dB at the design frequency [55].

4.2 Impact of Global Sidelobe Constraint on Frequency Re-use Antenna System

The interference between the different satellite communications systems has in the past been controlled by coordination such that any new system would not obstruct the existing systems. In the future, it likely that communications satellite antennas must meet reference pattern specifications similar to those which already apply to earth-station antennas and direct-broadcast satellite antennas. This will conserve the finite available frequency bandwidth and geostationary arc. Such antenna reference patterns are difficult to define for a contoured beam, which may be of a complicated shape. They will complicate the antenna design process as many more synthesis stations must be considered. This example investigates the potential impact of a global pattern envelope constraint on an antenna similar to the Intelsat VI 4-GHz hemi/zone antenna already considered in Section 2.2. This antenna already meets stringent sidelobe requirements in the adjacent frequency re-use coverage areas.

4.2.1 Sidelobe envelopes of current antennas

Figure 16 shows the calculated isogain contours at MCAG (the minimum coverage area gain) and 27, 30 and 33 dB below MCAG for the Intelsat VI Indian Ocean region (IOR) zone 2 beam at the lower edge of the 4-GHz band where the problems with sidelobes and the roll-off of the pattern from the coverage area are the most severe. The four spatially isolated zone beam coverages are indicated by the four piece-wise linear composite coverages. We note that fairly high sidelobes extend from zone 2 towards zone 4. The figure also shows a number of linear segments which extend from about 1° inside the zone beam coverage to about 7° outside. Figure 17 shows the superimposed cuts along these gain roll-off pattern traces. The horizontal angular scale gives the distance from the point where a gain roll-off pattern trace intersects the MCAG contour. No traces away from the Earth are considered. In these directions, the sidelobes are much higher. The full (dotted) line near 0° represents the maximum (minimum) envelope of the pattern traces. The full (dotted) line further away indicates the envelope of most (all) of the traces. The dot/dash line indicates the additional degradation caused by the calculated line length dispersion in the beam-forming network. In a practical antenna, several other imperfections will degrade the performance.

4.2.2 Gain roll-off optimization

Figure 18 indicates the location of the synthesis stations used in the optimization. Initially, no gain roll-off stations (indicated by 7) were used. The optimization then uses 176 stations and 36 beams. It is carried out at both band edges simultaneously so that the number of pattern constraints is twice the number of stations. Figure 19 shows the resulting gain contours at the lower edge of the band with isogain contours at the MCAG level and 27, 30 and 33 dB further down. The levels do not include losses and give directivity. The minmax solution is superior to the least-squares solution on the worst stations and improves in this case the MCAG level by 1.2 dB. The sidelobes are higher than in Figure 16 but the fit to the desired composite coverages is tighter.

Figure 20 shows the optimized gain contours obtained for carefully selected sets of gain roll-off stations. Initially, gain roll-off stations were set up from the edge of the composite coverage with a maximum tolerable field level calculated from a gain roll-off reference curve. This may lead to the specification of critical synthesis stations which with the minmax algorithm would destroy the overall antenna performance. With the gain roll-off curve used in the optimization, it was found that no gain roll-off station should be placed closer to the coverage area than 3° for this zone beam. Also, no stations should be placed in (the polar) regions where no feed is available for controlling the pattern. The resulting 265 synthesis stations are shown in Figure 18 with deleted gain roll-off stations marked by circles. The sidelobe performance has been considerably improved while the MCAG level has been reduced by only a few tenth of a dB. However, the gain slope of the edge of coverage has been degraded. Increasing the number of feeds slightly will improve the MCAG level and the gain slope but seem to have little impact on the sidelobe performance.

4.3 Reconfigurable Antennas with Shared Excitations

Increasing satellite lifetimes of 10 to 14 years have accelerated the need for the same spacecraft to be able to provide different services over different coverages at different times. The full range of possible future requirements to a spacecraft cannot be anticipated for such a long time and can probably only be met by a fully reconfigurable antenna system. Such antenna systems do not require any special synthesis software as the antenna may be optimized seperately for each coverage requirement. However, they are excessively complex and expensive to implement, and in practice, less complex and more reliable systems with limited reconfigurability are implemented, e.g., as in the Intelsat C-band hemi/zone antenna systems by means of switches. Such a case is considered in this section. A set of shared excitations is optimised to meet the Intelsat VI Atlantic and Indian Ocean region zone 2 beam coverage requirements. The shared excitations would then by switches be combined with sseparate sets of unique excitations for each ocean region. In each ocean region, the sidelobe requirements in the adjacent zone beam coverages are included.

Figure 21 and 22 show the 185 synthesis stations used for the Indian Ocean region zone 2 beam optimisation and the 218 synthesis stations used for the Atlantic Ocean region zone 2 beam optimisation. The minimum coverage area gain is optimized subject to meeting a sidelobe isolation of more than 30 dB in the adjacent zone beam coverages. First, the two zone beams will be optimised independently of each other. Then, the two zone beams will be optimised simultaneously sharing many element beams with identical excitations.

4.3.1 Optimisation with separate excitations

A initial optimisation is carried out for each coverage separately. Figure 23 and 24 show the contour plots of the two optimised zone beams. The optimisations are carried out using the analytic element-beam model. Isogain contours are shown through the minimum coverage area gain level and 20, 25, 30 and 35 dB further down. The minmax pattern error is slightly larger for Indian Ocean region zone beam.

4.3.2 Optimisation of shared excitations

At this stage, the two sets of excitations obtained by the optimization of each ocean region separately are inspected and each excitation is assigned to one of the following three BFNs:

BFN 1 generates the excitations only used by the Indian Ocean region zone beam,

BFN 2 which generates the excitations only used by the Atlantic Ocean region zone beam, and

BFN 3 which generates the excitations which are shared for the two zone beams.

The total number of element beams is 46. The breakdown of the element beams and the excitations between the two zone beams and the three BFNs is given in Figure 25. The combined synthesis problem consists of 61 different excitations and 403 synthesis stations. In this case, the synthesis is carried out so that the power division between BFN 1 and BFN 3 for the Indian Ocean region zone beam and between BFN 2 and BFN 3

for the Atlantic Ocean region zone beam are optimized by the program. Figure 26 and 27 show the contour plots of the two optimised zone beams with shared excitations for the analytic element-beam model. The minimum coverage area gain (or rather directivity) and the minimum sidelobe isolation are listed in Table 7 for the case with separate excitations and with shared excitations. The table gives date obtained both with tha analytic element beams and with element beams calculated by an accurate reflector analysis program.

	Analytic element beams		PO/GTD element beams	
	Separate	Shared	Separate	Shared
Min. gain:				
Indian 2	26.18 dBi	26.19 dBi	25.91 dBi	26.00 dBi
Atlantic 2	25.58 dBi	25.36 dBi	25.32 dBi	25.17 dBi
Min. isolation				
Indian 2	33.09 dB	33.10 dB	32.29 dB	32.55 dB
Atlantic 2	33.81 dB	33.10 dB	33.09 dB	32.55 dB

Table 7. Parformance with separate and with ahared excitations.

Thue, no degradation has takan place for the Indian Ocean region zone beam which had the largast minmax residuel. Tha performance of the Atlantic Ocean region zone beam has been "equalized" ao that minmax reeiduals now are identical for the two zone beams. The agreement between the reeults obtained by analytic beams and PO/GTD beams is eurprisingly good.

5 SHAPED CONTOURED-BEAM REFLECTOR ANTENNAS

In this Section we consider an alternative contoured-beam reflector antenne requiring only e single feed. The surface of the offset reflector is ehaped so that the modified wavefront elong the originel reflector surface provides the desired wevefront. The deviation from the paraboloidal surface ie so small that the amplitude distribution elong the originel reflector surfece remains essentielly undistorted end only negligible cross polarisetion is genereted. The similer surface sheping technique has previously been utilized for a jspanese experimental Ke-band communications satellite [56, 57].

5.1   Optimisetion of Aperture Phase Distribution

In our version of the synthesis technique, the phase of the aperture field is expanded into Zernike or circle polynomials, i.e.,

$$\Phi(\rho,\phi) = \sum_{n=1}^{N} \sum_{m=-n}^{n} c_{mn} a^{jm\phi} R_{mn}(\rho),$$ (34)

where ρ and ϕ are the poler eperture coordinates and $c_{-mn} = c_{mn}^*$. The Zernike or circle polynomiels find use in optics for orthogonal expansions in circuler epertures. The polynomials are simply releted to the scen aberrations such as spherical sberrations, estigmatism, coma, etc. [59]. Rapid celculation of circle polynomials is possible by recursion. The expansion coefficients c_{mn} take the role of the feed excitstions in the erray-fed reflector. For e particular set of expansion coefficients, the field is celculated on ell stations by e simplified and fast phyeicsl-optics integration ecross the deformed reflector surface. The ganeral minmax routine described in [47] is used to determine an set of expansion coefficients which optimise the gein on ell synthesis stations. The procedure hes eleo been utilised to synthesise ellipticel beams with very low sidelobes [58].

When en optimum phase distribution hes been detarmined, the shepad reflector is derived by e rey-treoing procedure from the offset paraboloid used as initiel solution. The optimisetion of the phase expansion coefficients is numericslly more difficult than feed excitation optimisation. The element beams are slmost orthogonel end verying one feed excitation affects only few stations. The phase expansion coefficiente, on the other hand, interact nonlinearly and vsrying one coefficient will affect all stetions but by very small amounts.

Tha reflector sheping procedure has been applied to the ECS coverage already considered in Section 4.1. The design wes cerried out et 11.2 GHs using the offset paraboloidal reflector similar to the one considered in Section 4.1 as starting point. An optimised surfece deformation which generetas the contoured beam is indicated by the three-dimensional plot in Figure 28. The optimised shaped reflector antenne system was enalysed by physical optics. Figure 29 shows the calculeted copolar isogein contours at the edges of the frequency band 1, 2, 3, 5, 10, 19, 20, 21 and 30 dB below peak gain. The calculeted minimum coverege eree directivity of 28.81, 29.21 and 28.84 dBi et 10.7, 11.2 and 11.7 GHs compare fevorsbly with the corresponding minimum coverage erea gain velues of 27.93, 28.18 and 28.10 dBi of the erray-fed reflector. No attempt wes made tc suppreee the sidelobes. The antenna was assumed to be circulerly polarised. The cross-poler performance wae found to be very sensitive to the cross-polar performance of the feed. Even low levels of feed cross polarisation would generate "hot spote" of cross polerisstion in the refleotor fer field.

5.2   Measurements on Shaped Contoured-beam Reflector

The ehaped reflector contouied-beam reflector wes re-optimised with e smaller offset angle θ_o to allow the use of a linearly polarised feed horn which wae aveilable. A modified aperture phase expaneion was determined with significantly lower sidelobes et the cost of a reduced minimum coverage area gain. The shaped reflector was manufactured for the scaled frequency band 16.4 - 18 GHs in order to reduce the reflector eiee to be within the limitations set by the eurfece machining equipment available. The antenna measuremente were carried out at the spherical near-field test range at the Technical University of Denmark. During the antenna measurements, the feed horn was found to move and it was necessery to

strengthen the feed support etructure. Figure 30 compares over an extended enguler renge the meeeured end the calculated co- and croee-poler pattern cuts along the planes of maximum end of minimum beamwidth. The agreement is excellent apart from the engular region $7^\circ < \theta < 14^\circ$ in the plane of the narrow beamwidth, where scattering from the enlarged faed support etructure appeers. The measured minimum coverege eree directivity of 27.3 dBi occurs at the high end of the band where the predicted velue ie 28.1 dB. The ehaped reflector antenna holds significent advanteges over the array-fed reflector antenne for applicetione where no reconfigurebility and only e eingle beam is required. No BFN ia required and complicated mutual coupling effecte in the feed array are evoided. The BFN end the epillover loeeee are absent or drestically reduced eo that the gain delivered cen be higher. Sheped reflector antenne systems ere in repid development end major future progress is likely with the recent edvent of rigoroue methode [60]. Work is aleo being carried out on duel reflectore [61].

6 DUAL REFLECTOR SYSTEMS WITH SMALL SCAN DEGRADATIONS

The duel offeet Cessegrain or Gregorian reflector systeme permit cancellation of the croee polerizetion for e linearly polarized on-exie beam [62]. This is echieved if the exas of the feed, the eubreflector end the main reflector are edjusted according to the condition

$$\tan \gamma/2 = 1/M \tan \psi/2 \tag{35}$$

where γ ie the engie from the main reflector axis to the subreflector exie end ψ the engle from the subreflector exis to the feed axie (see Figure 31). The velue of the eubreflector "magnificetion" M determines the eubreflector type:

(1) $M > 1$: The subreflector is the convex brench of e hyperboloid with the eccentricity
$\qquad$ $e = (M + 1)/(M - 1)$.
$\qquad$ Thie is a conventionel duel offeet Cassegrein.
(2) $0 < M < 1$: The subreflector ie the concave brench of e hyperboloid with
$\qquad$ $e = (1 + M)/(1 - M)$.
$\qquad$ This is either the front-fed or the side-fed duel offset Ceseegrain discussed below.
(3) $M < -1$: The eubreflector is an ellipsoid with
$\qquad$ $e = (M + 1)/(M - 1)$.
$\qquad$ This is e convantional dual offeet Gregorian.

Dual offset raflector configurationa which fulfil the condition (35) hea no first-order eetigmatism which otherwise ia the dominant acan eberration in offaet reflector antennes [30]. Conventionel compeneeted dual offset Cessagrain and Gregorian antennas, $M > 1$ and $M < -1$ above, are difficuit to design with no blockege for larga acan angles, and the faed errey ia lerger than in the ceae where the main reflector ia uaed ea single reflector. These problems are reduced when $0 < M < 1$ for tha two different configurationa in Figure 32, which both are designed for e $\pm10^\circ$ scan. In Figura 32a, the feed arrey is located in front of both tha subreflactor and the main raflector and the system haa baen tarmed it the front-fad offeet Cassegrein (FFOC) antenna system [63]. In the second configuretion in Figura 32b the feed array end tha subreflactor ara plecad on either sida of tha main raflactor. Thia system haa been termed the aide-fed offaet Cessagrain (SFOC) antenna ayatem [53]. Both the FFOC and tha SFOC have uniqua acan propertiaa ovar the full $\pm10^\circ$ fiald-of-view dua to tha larga focal langth of tha main raflactor. Tha large fiald-of-view requiraa thet tha subraflactor aiaa ba comparabla to tha main raflactor aiaa. For contiguoua Earth covaraga, tha faad array aiaa ia axcaaaiva and tha ayatema may not be competitiva to an array antenna. Howavar, tha inharent property of a raflector antenne ayetem of aaaociating aingla faeda with high-gain spot beama makea tha configurationa shown in Figura 32 vary attractiva candidataa for maating partial Earth coverage raquiramenta with many high-gain beama.

6.1. Scan Propertiaa of tha FFOC and tha SFOC

Figuraa 33 and 34 ahow tha calcuiatad principai co- and croaa-polar pattarn cuta for aacondary beama radiatad by amail linaarly polarisad conical horna placed at tha iocationa which ara corraaponda to beama on axis and with 10° downward acan, 10° upward acan and 10° latarel acan. Tha diametara of tha feeda ara 1.8λ (FFOC) end 2.2λ (SFOC) and corraapond to a beam apacing of 92 per cent of tha beam width. This ia cioaa to tha apacing which givaa tha highaat gain at tha croaa-ovar lavei for multi-beam applicationa whara each beam ia radiatad by a aingla horn. In each caae, the feed iocation ia optimiaed to minimiae tha phaea errora and tha feed axia ia aiignad ao that the cantral ray hita tha cantar of tha main raflector aurfaca. For both the FFOC and tha SFOC, tha diametar D of tha projectad apertura ia 120 λ. Tha amali feeda provida only a alight apartura tapar. Thia aituation exhibita both tha highaat aidaiobea and tha iargeat acan loaaea. Tha calcuiatad peak diractivity, peak aidaiobe lavei and peak aidalobe iavel for tha two configurationa ara givan in Tabla 8. Tha peak directivity ia broken up into a number of afficianciaa

$$G_{ac} = \eta_{ap} \, \eta_{ar} \, \eta_{ap} \, G_o \tag{36}$$

whera

$\qquad \eta_{ap}$ ia the apillovar efficiency, (tha fraction of the feed power which hits the main raflector),
$\qquad \eta_{ar}$ ia tha ralativa projectad area (the ratio of the areaa obtained by projacting the main raflector rim into a plana perpendicular to the direction of the acanned beam and into a plana perpendicular to tha direction of tha on-axia beam),
$\qquad \eta_{ap}$ ia tha apartura efficiency including loaa due to phaaa arrora, amplitude tapar and croaa polarization. (Thie loae in dominated by the phaaa arrora eaaociated with the acan as the aperture illumination ia almoat uniform), and
$\qquad G_o$ ia the peak echievable directivity $\pi D/\lambda$ (51.53 dBi for D = 120 λ).

Beam direction	η_{sp} dB	η_{ar} dB	η_{ap} dB	Directivity dBi	Sidelobe dB	Cross-pol dB
FFOC:						
on axis	-4.62	0	-0.03	46.88	-28.38	-48.68
10° downward	-3.48	+0.75	-2.28	46.52	-39.63	-38.06
10° upward	-5.87	-1.07	-1.55	43.04	-23.14	-35.52
10° sideward	-4.78	-0.07	-0.63	46.05	-33.63	-37.40
SFOC:						
on axis	-5.09	0	-0.02	46.42	-28.01	-54.78
10° downward	-4.68	+0.34	-0.36	46.83	-33.28	-40.20
10° upward	-5.72	-0.52	-0.24	45.05	-29.88	-37.49
10° sideward	-5.29	-0.07	+0.03	46.20	-30.25	-41.56

Table 8. Peak directivity budget and peak sidelobe level of FFOC and SFOC.

Due to the relatively small feed size and small angle subtended by the subreflector rim, the feed
spillover is large. The large scan causes a significant change of the relative projected area. As the main
reflector is closer to vertical for the SFOC than for the FFOC, the area loss for upwards scan is smaller
for the SFOC. The aperture efficiency is, except for the on-axis beam, dominated by phase errors, i.e.,
scan aberrations. We see that the affect of these phase errors is smaller for the SFOC. The smaller scan
aberrations of the SFOC also follow from the pattern in Figures 33 and 34. The sidelobes and the cross
polarization are lower for the SFOC than for the FFOC. As the aperture diameter increases, e.g., to 240λ,
the superiority of the SFOC with respect to electric performance is accentuated. For both configurations,
the scan losses are higher for beam scanning in the plane of symmetry than in the perpendicular plane. In
the plane of symmetry, the scan losses due to phase errors are slightly higher for downward scan, but they
are compensated by reduced spillover and area losses. In a practical design, the antenna axis should be
repointed to equalize the overall scan loss in all directions or give preference to critical areas in the
coverage. Comparisons with the single offset paraboloidal reflectors show that the FFOC achieves similar
scan performance as a single offset parabole with an f/D ratio equal to about 2.6. The SFOC is comparable
to a single offset parabole with an f/D of about 5.6.

More details including the initial design of a feed array to generate 10 contoured beams out of the
SFOC are given in [53].

7   CONTOURED-BEAM ARRAY ANTENNAS

Table 2 indicated the significant growth of the feed array size for each new INTELSAT spacecraft
series. If the trend towards larger end radiating apertures and f/D ratios continues, the feed array sizes
will ultimately exceed the reflector size and the antenna mass and volume requirements will have a
tremendous impact on spacecraft design and launch cost. Thus, it may become advantageous to "discard the
reflector and turn the feed array towards the Earth" and use it as a directly radiating array.

7.1   Array Excitation Optimisation with Pencil Element Beams

We consider the planar array configuration in Figure 35. It consists of N_a elements in a hexagonal
lattice. We define N_b element beams radiated by the array in a hexagonal lattice over the field-of-view
shown in Figure 36. The half-power beamwidth of the element beams is determined by the array diameter D
and is for a uniform array illumination approximately $\Delta\theta_3 = \lambda/D$. The optimization of the array excitations
to meet specified coverage and isolation requirements is carried out by the algorithms discussed in
Section 3 but indirectly by optimizing the excitations of the element beams. Then, the array excitations
are calculated from the element-beam excitations. The optimisation via the element beams is much more
efficient than a direct optimisation of the array excitations because

(1)   the number of element beam is in general much less than the number of array elements, and
(2)   the element beam are almost orthogonal to each other over the far-field pattern in the sense
      their pattern only overlap little as opposed to the array element patterns, which overlap
      completely. As a result, the optimisation is a more well behaved problem.

The number of array elements for a given aperture size is determined by the requirement that no grating
lobes fall in the field-of-view. The antenna designer may choose the element-beam positions independently
for each coverage area of a multi-beam array antenna. This is not possible for a reflector antenna. The
aperture size in wavelengths and the angular extent of the coverage area determines the number of the
degrees of freedom of the synthesis problem [64]. In most cases, the beam spacing can be chosen a little
larger than the beam width as in the case of a reflector antenna. No advantages are gained by choosing the
beam spacing significantly smaller than the beam width.

Figure 37 shows an optimised contoured beam for an array consisting of 169 conical horns with a
diameter of 2.84 λ. The array diameter is identical to the size of the INTELSAT VI hemi/zone reflector. By
gradual removal of weakly excited array elements followed by re-optimisation of the remaining excitations,
the number of array elements can be reduced significantly. A full account of the design procedure and many
design cases have been given in [65].

8.   ACKNOWLEDGEMENTS

9 REFERENCES

[1] "Radio Ragulations", ITU, Ganeva, 1982

[2] KG Schroader (1972), "Charactaristics and applications of multi-baam spacecraft antennas", 4th AIAA Comm. Sat. Syst. Conf., Washington, D.C., paper No. 72-530

[3] P Foldae (1982), "Recant advances in multibaam antsnnas", 11th European Microwavs Conf., Amstardam, 59-72

[4] LJ Ricardi (1982), "Multiple baam antannas", Ch. 6 in AW Rudga, K Milns, AD Olver and P Knight (Eds.), "The Handbook of Antanna Dasign. Volume 1". London: Patar Paragrinue Ltd.

[5] JL Butlar (1966), "Digital, matrix and intsrmediate-frequancy acanning", Ch. 3 in RC Hansen (Ed.), "Microwava Scanning Antennas. Volume 3". Naw York: Academic Press, 241-268

[6] AR Dion (1982), "Lsns antennae", Sact. 3.7 in AW Rudge, K Milns, AD Olver and P Knight (Eds.), "The Handbook of Antanna Daeign. Volume 1". London: Petar Paragrinus Ltd.

[7] HHS Luh, TM Smith and WG Scott (1982), "A dual-band TEM lens for a multipls baam antanna", IEEE Trans. Antennas Propagat., Vol. AP-30, 224-229

[8] F Taormina, DK McCarty, T Crail and D Nakatani (1976), "INTELSAT IVA communications antenna - frequancy ra-uee through spatial isolation", Intl. Conf. on Communicationa, Philadalphia, 4.10-4.14

[9] CC Han, AE Smoll, HW Bilanko, CA Chuang and CA Klein (1976), "A beam-shaping multifaed offsat reflactor antanna", 6th AIAA/CASI Comm. Sat. Syet. Conf., Montreal, 245-249

[10] EW Matthewe, CL Cuccia and MD Rubin (1979), "Technology considerationе for tha use of multiple baam antenna eystems in communications satallites", IEEE Trane. Microwava Theory Tech., Vol. MTT-27, 998-1004

[11] MF Caulfisld, FA Taormina, BM Flynn, SO Lane, TM Paige and VE Cascia (1982) "INTELSAT VI antanna syetam design and development", ConF. Large Spacs Antsnna Syst. Tech., NASA Langlay, 743-765

[12] SO Lane, MF Caulfield and FA Taormina (1984), "INTELSAT VI antanna system overview", 10th AIAA/CASI Comm. Sat. Syst. Conf., Orlando

[13] WJ English (1980), "Improving future communications satsllita antanna daeigna", 8th AIAA/CASI Comm. Sat. Syst. Conf., Orlando, 464-470

[14] DF DiFonzo (1982), "Evolution of eatellite antennaa", IEEE Intl. Symp. Antannse Propagat., Albuquerqua, 358-361

[15] P Nayrat (1984), "Antenna tachnology at INTELSAT", Journéae Internationalse ds Nica sur les Antannae, Nica, pp. 69-90.

[16] WVT Ruach (1982), "Rsflectore with contoured beams", Sect. 3.5 in AW Rudge, K Milns, AD Olver and P Knight, "Tha Handbook of Antanna Deaign. Volume 1". London: Pater Paragrinus Ltd.

[17] B Vidal Saint Andre and P Neyrst (1980), "Tha application of single raflactor multi-feed antennae to direct T.V. satallitas", 10th European Microwave Conf., Warazaw, 90-94

[18] A Roedarar(1984), "Antannaa pour satellite de télévision directa", Journées Internationales ds Nica sur las Antannes, Nica, 154-167

[19] H Soule, J Rosan, J MacGahan, J Dumae and C Profars (1984), "Shapad-baam antenna for direct broadcast satsllitss", 10th AIAA/CASI Comm. Sat. Syst. Conf., Orlando

[20] V Galindo-Israal, Y Rahmat-Samii, W Imbriala, H Cohan and R Cagnon (1984), "A CONUS tima zone DBS antanna system with einqle polarisation", IEEE Intl. Symp. Antennae Propagat., Boston, 143-146

[21] K Pontoppidan (1979), "Pattarn pradiction methods for high performance single and dual raflector antennaе", Final Report S-101-02 on ESTEC Contract 3629/78/NL/AK, TICRA A/S, Copanhagsn, Danmark

[22] SW Laa and Y Rahmat-Samii (1981), "Simpla design formulas for dasigning an offsat multibaam parabolic raflactor", IEEE Trane. Antennss Propagat., Vol. AP-29, 472-478

[23] A Ssitto (1981), "Gain-bandwidth product and othar raflector antenna relationships", ESA Journal, Vol. 5, 249-258

[24] GAE Crons, A Jorgansen and A. Roedarar (1984), "Comparison of contoured beam rsflector antenna dasiyns for improvad European covarage", IEEE Intl. Symp. Antennas Propagat., Boston, 792-795

[25] PD Patal and KK Chan (1985), "Optimization of contoured beams for satallite antennas", Proc. IEE, Vol. 132, Pt. H, 400-406

[26] Y Rahmat-Samii and SW Laa (1983), "Directivity of planar array faeds for satellite raflactor applications", IEEE Trans. Antennas Propagat., Vol. AP-31, 463-470. Sae also corrwction in Vol. AP-32, 762

[27] PJB Clarricoats, SM Tun and CG Parini (1984), "Effacts of mutual coupling in conical horn arrsys", Proc. IEE, Vol. 131, Pt. H, 165-171

[28] L Lewin (1975), "Exprassion for dacoupling in multiple-beam antennas", Elsctr. Ltrs., Vol. 11, 420-421

[29] PJ Wood (1986), "Some sxtsnsions of tha beam orthoyonality concapt for multi-beam antsnnas", IEEE Montech '86 Conf. Antennas & Comm., 310-313

[30] C Dragona (1982), "A first-ordar trastment of aberrations in Cassagrainian and Gragorian antennas", IEEE Trans. Antennas Propagat., Vol. AP-30, 331-339

[31] J Ruza (1965), "Lataral-feed displacement in a paraboloid", IEEE Trans. Antennas Propagat., Vol. AP-13, 660-665

[32] TS Chu and RH Turrin (1973), "Depolarisation propertias of offsat raflector antennas", IEEE Trans. Antennas Propagat., Vol. AP-21, 339-345

[33] NA Adatia and AW Rudge (1975), "Beam-squint in circularly polarisad offset raflactor antennas", Elsctr. Ltrs, Vol. 11, 513-515

[34] EA Ohm (1979), "Multibeam satellits antenna with optimised polarisation distribution and full U.S. coverage", IEEE Intl. Symp. Antennas Propagat., Saattle, 266-269

[35] J Jacobsan (1977), "On the cross polarisation of asymmetric reflector antennas for satellite applications", IEEE Trans. Antannas Propagat., Vol. AP-25, 276-283

[36] MJ Gans and RA Semplak (1975), "Some far field studias of an offset launcher", BELL Syst. Tech. J., Vol. 54, 1319-1340

[37] TS Bird (1982), "Contoured-beam synthesia for array reflector antennas by fiald correlation", Proc. IEE, Vol. 129, Pt. H, 293-298

[38] JF Bull, P Kalata and CE Profera (1982), "Application of the method of steepest descent optimization to tha design of shaped beam antennas", IEEE Intl. Symp. Antennas Propagat., Albuquerque, 600-603

[39] C Dedeban, M Minoux and P Brachat (1984), "Un logiciel pour l'optimisation du diagramme de rayonnement d'une antenne à faisceau conforme", Journées Internationales de Nice sur las Antennes, Nice, 56-63

[40] S Mano, T Katagi and T Tsutsumi (1984), "Pattern synthesis of array fed reflector antennas", Electronica and Communications in Japan, vol. 67-B, No. 7, 38-45

[41] K Shamsaifar and M Calvo (1986), "Contoured beam synthesis for a small number of feeds by optimising their position and excitation", IEEE Intl. Symp. Antennae Propagat., Philadelphia, 727-730

[42] RFE Guy (1985), "A synthesis technique for array antennas of general shape with various aperture constraints", 4. Intl. Conf. Antennas Propagat., Warwick, 35-39

[43] GT Poulton (1986), "Antenna power pattern synthesis using method of successive projections", Elactr. Ltrs., Vol. 22, 1042-1043

[44] AI Zaghloul and DK Freeman (1986), "Phased array synthesis for shaped beams using power matrix method", IEEE Intl. Symp. Antennae Propagat., Philadelphia, 177-180

[45] D Kawabata, M Uano, T Morroke, T Chiba, R Kawashima, W Bornemann and WJ English (1986), "Synthesis of spacecraft antennas by use of Fourier transform method", IEEE Intl. Symp. Antennas Propagat., Philadelphia, 719-722

[46] JR Mautz and RF Herrington (1975), "Computational methods for antenna pattern synthesis", IEEE Trans. Antennae Propagat., Vol. AP-23, 507-512

[47] K Madeen (1975), "Minimax solution of non-linear equations without calculating derivatives," Math. Prog. Study, Vol. 3, 110-126

[48] CG Broyden (1965), "A class of methods for solving non-linear simultaneous equations", Mat. of Comp., Vol. 19, 577

[49] K Madsen and H Scheer-Jacobsen (1976), "Singularities in minimax optimization of networks", IEEE Trans. Circuits and Systems, Vol. CAS-23, 456-460

[50] CA Klein (1984), "Design of shaped-beam antennas through minimax gain optimisation", IEEE Trans. Antennas Propagat., Vol. AP-32, 963-968

[51] L Deemen (1986), "Etude d'optimisation d'antennes multisources", M.Sc.EE Thsais, Faculté des Sciencas Appliquées, Univareité de Liège

[52] P Foldes, F Rispoli and R Jorganeen (1986), "Antenne design for the Eutalset program", IEEE Intl. Symp. Antennas Propagat., Philadelphie, 165-168

[53] R Jorgensen, P Balling end WJ Englieh (1985), "Dual offset reflector multi-beam entanne for international communications satellite applications", IEEE Trans. Antennas Propag., Vol. AP-33, 1304-1312.

[54] S Adatie, P Salling, S Claydon, P Ingvarson end A Roederer (1980), "A European contoured beam reflactor antenne development", 10th European Microwava Conf., Warsaw, 95-99

[55] DJ Brain, A Brunt, WT Costello, Y Kol, MS Sidat end R Waugh (1985), "A circularly-polarised antenna for contoured beam coverage of Europe", 4th Intl. Conf. Antennae Propagat., Norwich, 536-540

[56] T Ketagi and Y Takeichi (1975), "Shaped-beam horn reflector antenna", IEEE Trans. Antennas Propagat., Vol. AP-23, 756-763

[57] H Kumasawa, T Katagi and T Ebisui (1983), "Shaped-beam horn reflector antennae with eparture phase distribution modified by a plane wave", IEEE Intl. Symp. Antennae Propagat., Houston, 338-341

[58] R Jorgansen (1980), "Coverage shaping of contourad-beam antennae by aperture field synthesis", Proc. IEE, Vol. 127, Pt. H, 201-208

[59] S Cornblaat (1976), "Microwave Optics". London: Academic Press, 380-383

[60] BS Westcott (1983), "Shaped Reflector Antenna Design". Letchworth, Hertfordshire, England: Research Studies Press Ltd.

[61] N Adatia and S Tun (1986), "Shaped dual offset reflector antennas for contoured beam spacecraft applications", Journées Internetionelae de Nice sur les Antennas, Nice, 148-153

[62] H Taneka and M Nieuesws (1975), "Elimination of cross-polarisation in offset dual-reflector antennae", Electronics and Communications in Japan, Vol. 58-B, No. 12, 71-78

[63] S Makino, Y Kobayashi, S Urasaki and T Ketagi (1984), "Front fed offset Cassegrain type multibeam antenna", National Convention of IECEJ

[64] JT Mayhan (1976), "Nulling limitations for a multiple beam antenne", IEEE Trans. Antennas, Propagat., Vol. AP-24, 769-779

[65] W Bornemann, P Balling end WJ English (1985), "Synthesis of spacecraft array antennas for Intelset frequency reuse multiple contoured beams", IEEE Trans. Antennas Propagat., Vol. AP-33, 1186-1193
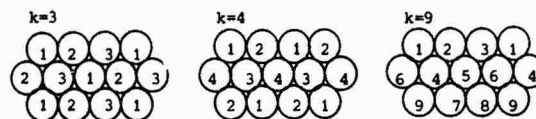
Figure 1   Multi-beam beam topologies for frequency re-use.

offset reflector

Earth

Feeds

BFN

Beam port A
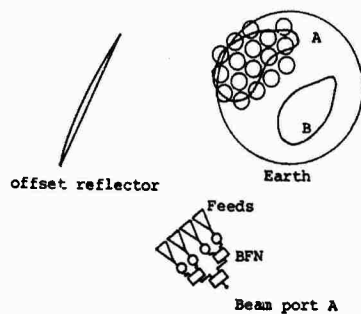
Figure 2   Contoured beam from offset reflector with
feed array and BFN

Feeds

Feeds

Bootlace lens   zoned waveguide lens
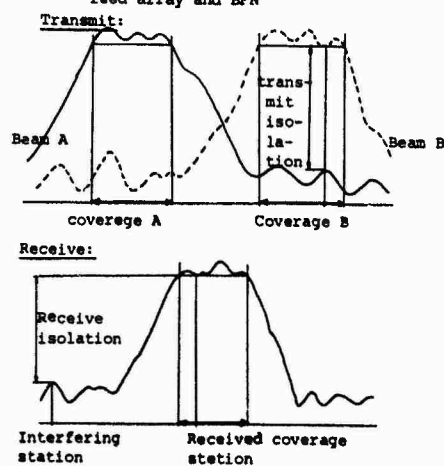
Figure 3   Microwave multi-beam lens antennas

Transmit:

Beam A

transmit isolation

Beam B

coverege A   Coverage B

Receive:

Receive isolation

Interfering   Received coverage
station   station

—— hemi beams (RHCP at 4 GHz)
--- zone beams (LHCP at 4 GHz)

VI:
Atlantic Ocean:

V:
Atlantic and
Pacific Ocean:

Indian Ocean:

IV A:
All Oceans: Indian Ocean:

Pacific Ocean:

Figure 5   Growth in the complexity of the INTELSAT
spacecraft hemi/zone coverages

Figure 4   Definition of isoletior for transmit and
receive contoured-beam antennas.

area in square degrees

peak achievable gain G_o in dBi

Figure 6   Contoured-beam efficiencies versus
coverage area size for 3.2 m reflec-
tor at 4 GHz. The lines are determined
by linear regression for the following
three cases:
—·— INTELSAT VI antenna (●●)
---- similar but with 1.3λ feeds (●●)
-·-· similar but with 1.3 feeds and
relaxed coverage area space. (oo)

$D=2a$

$d_1=d_c+a$
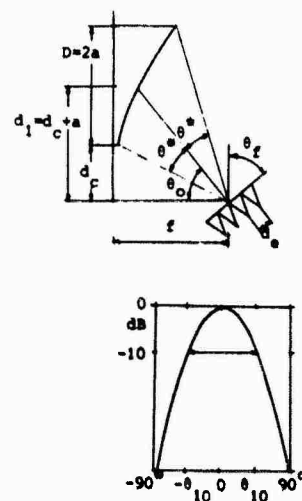
Figure 7   Reflector and feed parameters used
in the simple analytic beam model.
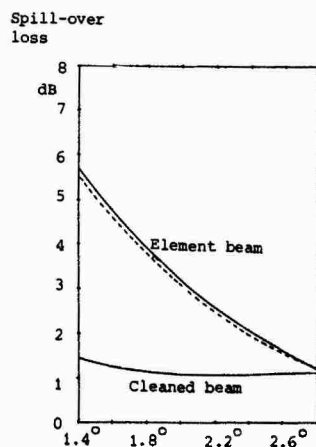
Spill-over
loss

Figure 8   Spillover loss vs. spacing of com-
ponent beams.
———— simple analytic beam model
---- reflector antenna analysis program
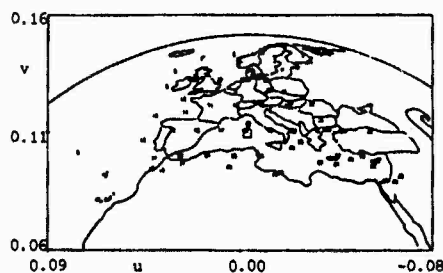
Figure 10   Examples of discrete stations (or sampling
points) representing coverage-area specifi-
cations.

Figure 11   Contour plots for best analytical beam
configuration   ➡

Sideview of array-fed
offset reflector
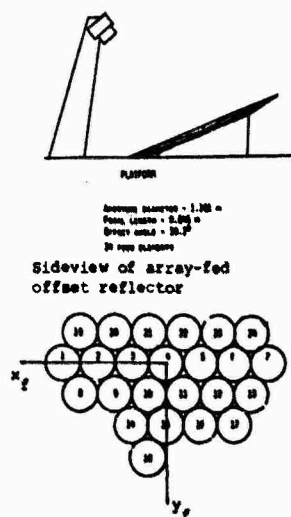
Figure 12   Initial ECS contoured beam reflector
and feed array

Figure 13   PO/GTD element beams and contoured
beam at 10.7 GHz   ➡
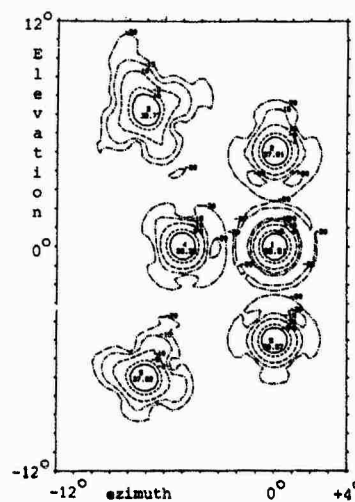
Figure 9   Gain contours 1, 3, 5, 10, 15 and 20 dB
below peak gain level for on-axis and
scanned element beams in a 43λ diameter
offset-fed paraboloid.
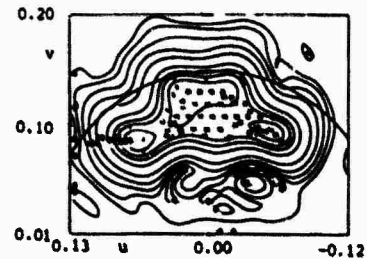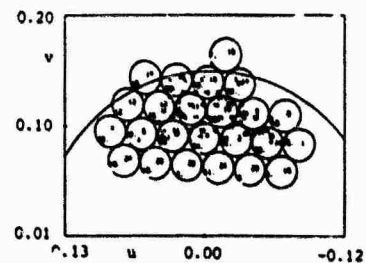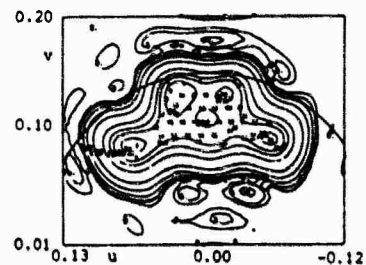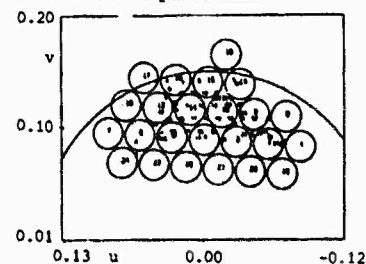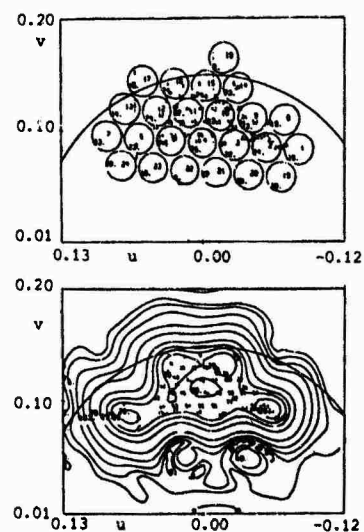
Figure 14 PO/GTD element beams and contoured beam at 11.7 GHz
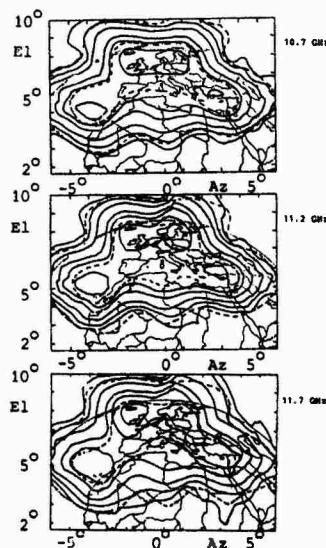
Figure 15 Measured gain contours 1, 3, 5, 10, 15 and 20 dB and calculeted gain contours 3 and 20 dB below peak gain for ECS coverage erray-fed contoured-beam reflector antenna
—— measurements (ERA)
----- calculetion
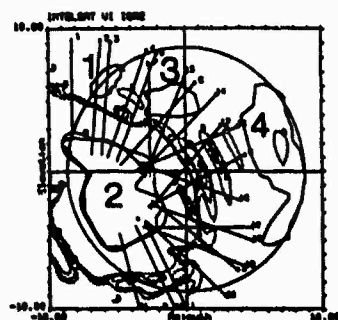
Figure 16
Nominel I-6 IOR zone 2 contours
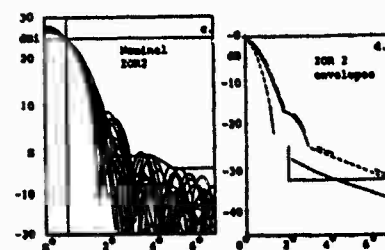
Figure 17 Gain roll-off patterne trecee and envelopes ofr I-6 IOR zone 2.

Figure 18
IOR 2 synthesis stations
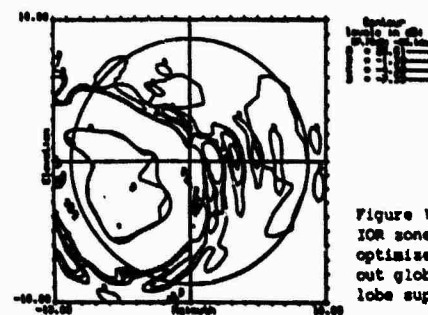
Figure 19
IOR zone 2 beam optimized without global sidelobe suppression
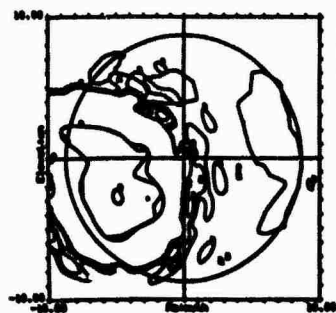
Figure 20
IOR zone 2 beam optimized with global sidelobe suppression
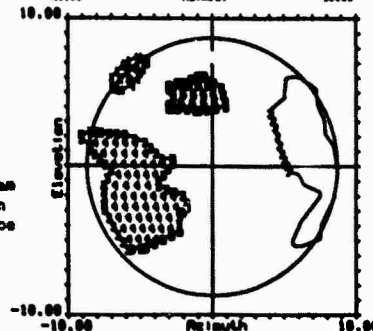
Figure 21
Synthesis stations for Indian Ocean region zone 2 beam
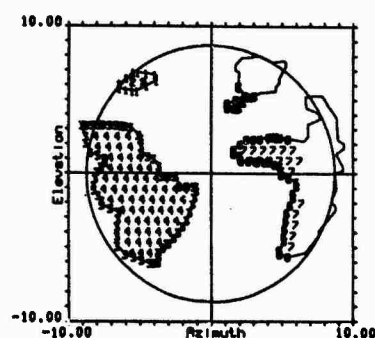
Figure 22   Synthesis stations for Atlantic Ocean
region zone 2 beam

Figure 23
Indian Ocean re-
gion zone 2 beams
optimized sepa-
rately

Figure 24
Atlantic Ocean re-
gion zone 2 beams
optimized separa-
tely
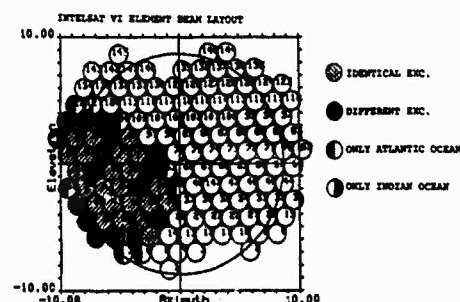
Figure 25   Shared and separate excitations for
Indian and Atlantic Ocean region 2 beams

Figure 26   Indian Ocean region zone 2 beam opti-
mized with 23 feeds common with Atlan-
tic Ocean region zone beam
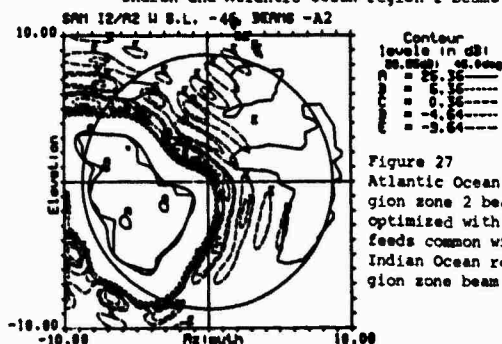
Figure 27
Atlantic Ocean re-
gion zone 2 beam
optimized with 23
feeds common with
Indian Ocean re-
gion zone beam

Figure 28   Deviations Δz of shaped reflector
surface from paraboloid.

Figure 29   Isodirectivity curves for shaped
reflector at edges of frequency band.
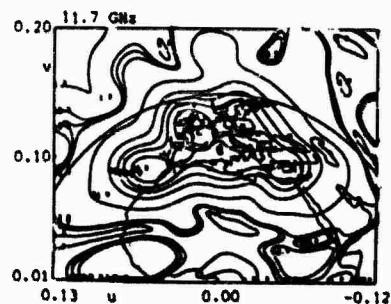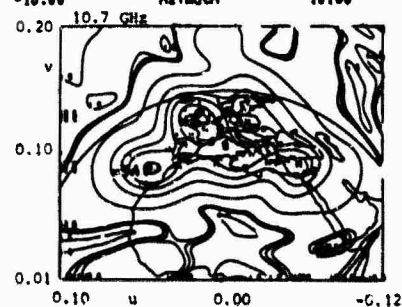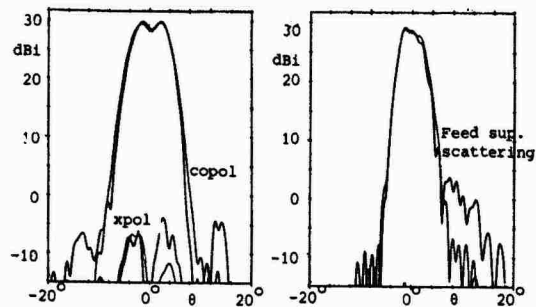
Figure 30 Measured and calculated principal pattern cuts at 11.7 GHz for shaped contoured-beam reflector.
———— measurement (TUD)
----- calculation
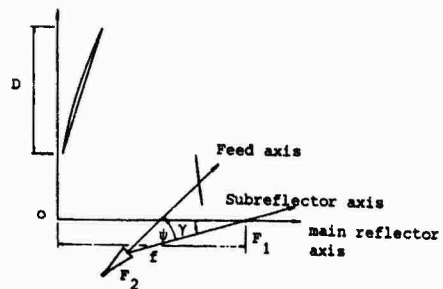
Figure 31 Conventional dual offset Cassegrain compensated for cross polarization and astigmatism

a. FFOC: b. SFOC:
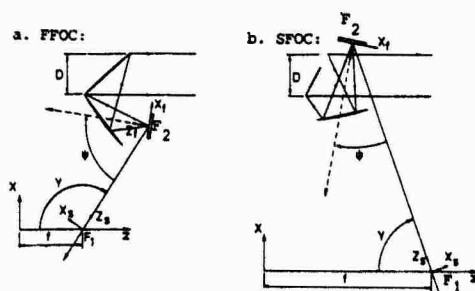
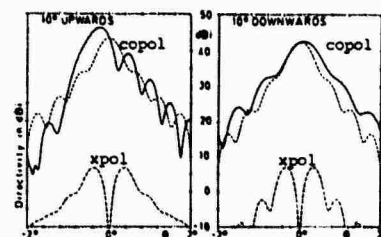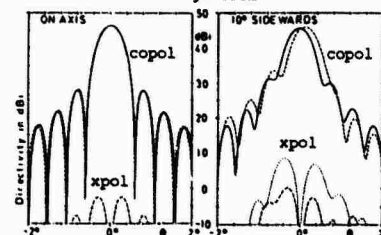Figure 32 Alternative dual offset Cassegrain antennas compensated for cross polarization and astigmatism

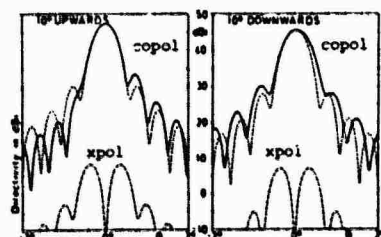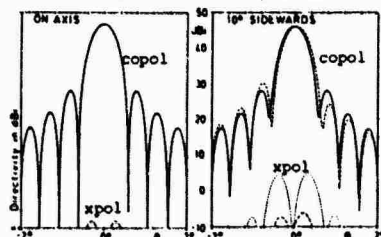Figure 33 Principal pattern cuts for element beams in 120λ FFOC.

Figure 34 Principal pattern cuts for element beams for 120λ SFOC.

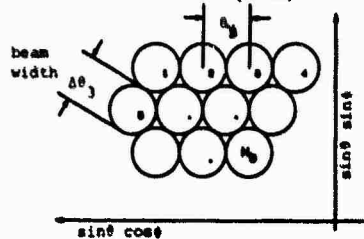Figure 35 Array antenna element configuration

Figure 36 Array antenna element beams

Levels:
———— -1 dB
········· -3 dB
———— -5 dB
—·—·— -10 dB
—··—·· -20 dB
—···—··· -25 dB
———— -30 dB

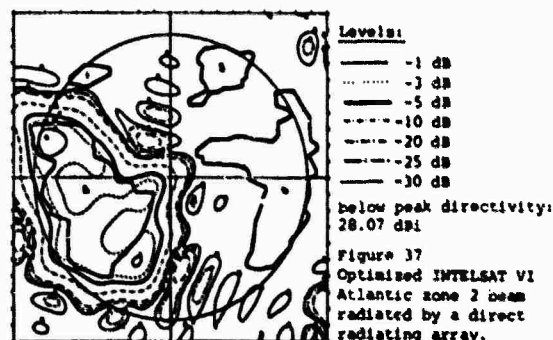below peak directivity:
28.07 dBi

Figure 37 Optimized INTELSAT VI Atlantic zone 2 beam radiated by a direct radiating array.